STELLAR CHARACTERISTICS

INTRODUCTION

Stars are arguably the most important single structures in the Universe. Their formation by gravitational collapse of gas and dust in the hearts of cool, giant molecular clouds may spawn additional bodies like planets, asteroids, and comets, while their demise may help to initiate subsequent waves of star formation. The nuclear furnaces buried deep in the cores of stars provide the energy which illuminates them but also create from initial stores of hydrogen and helium all the heavier chemical elements that have made life as we know it possible. Increasingly larger aggregates of stars produce a hierarchy of cosmic entities--binary and multiple stars, galactic and globular clusters, galaxies, and clusters of galaxies--whose structure, evolution and dynamics are influenced, if not determined, by the mass and motion of their constituent stars. Little wonder then why scientists and engineers engaged in astronomical work, regardless of their particular area of specialization, strive to develop a good appreciation for the basic properties of stars.

In what follows, the focus of attention will be on information about the characteristics of "normal" stars gleaned primarily through the study of the optical light they emit. There is no doubt that significant advances in our understanding of some stars (for example, compact stellar endpoints in binary systems, extremely hot and luminous stars, and young stars newly formed from the interstellar medium) have come through investigations of the radiation they produce in the X-ray, ultraviolet, and radio portions of the electromagnetic spectrum. However, for the vast majority of stars in the Galaxy which emit predominantly in the visible region of the spectrum, data from these other regimes constitute "the icing on the cake" as opposed to the substance of the basic layers. Additional information about stars is also potentially available from non-photon sources like gravitational radiation and cosmic rays, but the contribution to our knowledge of normal stars from these channels is too small at present to consider in a brief article like this one.

DISTANCES AND BRIGHTNESS

To fix the true brightness of a star, we need to know its distance. The most fundamental way of assessing stellar distances is by an application of the surveyor's method of triangulation, called *trigonometric parallax*. Figure 1 shows this technique schematically in the simplest possible case of an otherwise stationary star lying in the plane of the Earth's orbit (the *ecliptic plane*). Basically, one measures the angular shift in the position of the star relative to more distant, "fixed" reference stars on images taken from two widely separated locations. In the limit of small angles (which almost always holds in astronomical circumstances), the *parallax*, p, thus determined is related to the (perpendicular) distance, d, and the separation, D, between the observing points by:

$$d = 0.5D / p,$$

where p is measured in radians. As applied in astronomy, this formula is modified to take account of the facts that the baseline for observation has traditionally been the diameter of the Earth's orbit about the Sun, and the units of angular measurement usually employed are seconds of arc (1 radian = 206265 arcseconds). The mean distance separating the Earth from the Sun is, by definition, 1.0 astronomical unit (AU; 1 AU = 1.496×10^{11} m). With these substitutions, the equation above reduces to:

$$d = 206{,}265 / p,$$

with p now measured in arcseconds and d in AU.

This expression prompts the definition of a new unit of distance. Specifically, the *parsec* is defined as the distance to a star whose *par*allax is 1.0 arc*sec*onds. Thus, 1 parsec (pc) = 206,265 AU = 3.26 light-years = 3.085×10^{16} m. With this change, the equation relating distance in parsecs to the parallax angle in arcseconds becomes simply

$$d = 1 / p.$$

Because stars (excluding our own Sun) are so far away, none has a parallax angle greater than 1.0 arcsecond. Indeed the nearest star, α Centauri C, has a parallax of 0.77 arcseconds and a distance of 1.30 pc.

Older parallax measures were made with long focal length refracting telescopes and photographic plates; the best precision achievable by these techniques was ~0.01 arcseconds, yielding a maximum distance of about 100 pc. Modern measures, made with CCD detectors aboard satellites like Hipparcos, can be made to the nearest 0.001 arcseconds or better, thereby reaching distances of more than 1000 pc. Prior to the publication of the Hipparcos data in 1997, there were perhaps a few hundred stars with distances known to 5% or better; the number of stars with

distances having this level of accuracy is now about 7000. Even this advance is but a small step out into the Galaxy, however, whose diameter is some 30,000 pc. Clearly, astronomers must have other weapons in their arsenal to be able to assess the distances to even more remote stars, and some of these will be discussed later. An important point to make, however, is that all other distance-determining techniques employed by astronomers are calibrated upon and draw their accuracy from the fundamental method of trigonometric parallax.

Once the distance to a star is known, its intrinsic brightness or *luminosity* (total emitted energy per time) may be obtained from measurements of its apparent brightness using the inverse square law of light. Except for observations made in wavebands outside the visible (like the radio, X-ray, or ultraviolet) where actual flux measurements are typically reported, stellar brightnesses are usually given in terms of magnitudes, a practice which dates back to the ancient Greek astronomers. Under this system in its modern conception, the magnitude, m, of a star is logarithmically related to the received flux (energy per area per time), f, as follows:

$$m \propto -2.5 \log f.$$

The minus sign ensures that the larger the flux, the smaller the stellar magnitude, consistent with the way in which the system was originally introduced in second century BC by Hipparchus. Thus, the difference in magnitude between two stars or between measurements of the same star in two different bandpasses becomes:

$$m_1 - m_2 = -2.5 \log (f_1 / f_2).$$

Clearly, equal differences in magnitude correspond to equal flux ratios anywhere along the scale. Table 1 gives the observed magnitudes for some of the brightest appearing stars in the sky.

The measured fluxes typically represent the convolution of the flux from the star, f_*, (ignoring for the moment any modifications due to the intervening interstellar medium) reaching the Earth with the sensitivity (or efficiency), E_λ, of the instrument used to make the observations, including the bandpass characteristics of any filters employed, and, if the measurements are made from the Earth's surface, the ubiquitous effects of absorption in the atmosphere as a function of the position of the star in the sky, κ_λ. Thus,

$$f = \int f_* \bullet E_\lambda \bullet \kappa_\lambda \, d\lambda.$$

Formally, the integral is over all wavelengths, but in actuality, it only extends over the wavelength range for which the instrumental response is appreciably greater than zero. Presumably, the instrumental sensitivity is known, having

been determined in the lab by standard photometric techniques; the effects of the Earth's atmosphere, if present, may also be modeled given the (known) zenith angle of the observations and the transparency of the atmosphere as a function of wavelength (see Figure 2). Thus, in principle, the extra-atmosphere flux may be established for any stellar source.

In practice, what has been done is to establish a network of standard stars distributed conveniently across the sky for a variety of filter systems to permit the rapid and accurate calibration of instrumental systems and reduction of brightness measurements to standard magnitudes. The various systems in use today reflect the needs of astronomers to ascertain information about a star's temperature, gravity, and chemical composition. Table 2 lists some of the properties of a number of common filter/magnitude systems.

Application of these different filter systems frequently involves considering the differences between the observed or *apparent* (as in "appearing") brightness of a star in two bandpasses. The *color index* or simply the *color* of a star is what astronomers call such differences. Thus, in the *UBV* (Johnson) system, one has the *(B - V)* color or color index:

$$(B - V) = -2.5 \log (f_B / f_V),$$

where f_V and f_B are the extra-atmosphere fluxes observed with the *V* and *B* filters, respectively. Similarly, in the Strömgren system, one has the $(b - y)$ color defined by

$$(b - y) = -2.5 \log (f_b / f_y).$$

The color of a star can be related to its temperature. In the simplest of models where the star is assumed to be a perfect, or *blackbody*, radiator, the $(B - V)$ color can be used to establish the approximate temperature of a star as follows:

$$(B - V) = 7000 \, (1/T - 1/10{,}000),$$

where, in the Johnson system, a star of temperature 10,000 K is defined to have $(B - V) \cong 0.00$. The significance of such *color temperatures* is that, from stellar atmosphere theory, they can be related to fundamental parameters like the luminosity (see below) and the *surface gravity*, *g*, of the star.

This is just one example of the utility of brightness measurements for establishing the basic characteristics of stars. There are many more. For instance, colors in the Strömgren system may be used to effectively identify stars with high luminosity or with strong metallic line absorption indicating chemical compositions that differ substantially from that of the Sun and most other "normal" stars.

Returning now to the issue of distance, we recognize that the fluxes described so far are the observed fluxes arriving at the top of the Earth's atmosphere, not those associated with the surfaces of the stars. To recover from the apparent magnitudes a measure of the intrinsic brightness of the star, we must know the distance to the star. Replacing the received flux by the intrinsic flux, f_0, using the inverse square law of light, and recognizing that the energy released by the star is distributed over a sphere of area $4\pi d^2$, where d is the distance, we obtain

$$m \propto -2.5 \log f_0 / 4\pi d^2 = 5 \log d - 2.5 \log f_0 / 4\pi.$$

Astronomers have found it convenient to define the *absolute magnitude* M of a star to be the apparent magnitude it would have <u>if</u> its distance from us were 10 pc. In this case, we may write

$$M \propto -2.5 \log f_0 / 4\pi (10)^2 = 5 - 2.5 \log f_0 / 4\pi,$$

or

$$m - M = 5 \log d - 5 = 5 \log (d / 10),$$

since in a given photometric system the proportionality constants will be the same for both apparent and absolute magnitudes.

The quantity $(m - M)$ is called the *distance modulus*, and is directly proportional to the distance to the star. If m is measured and d is known (from parallax measurements), then M may be found. If, on the other hand, m and M are available (an alternative way of assessing M will be given later), then the distance to the star may be inferred. The distance modulus may be defined in any of the various filter systems introduced earlier. So, for example, in the *UBV* system with $m \Rightarrow V$ and $M \Rightarrow M_V$, one may consider the visual distance modulus, $(V - M_V)$. The relationship between m, M, and d is one of the most fundamental in all of stellar astronomy.

In formulating our discussion so far, we have ignored any possible effects due to the absorption of radiation by the interstellar gas and dust arrayed along the line of sight to the star. This correction, which varies with wavelength,

can be folded in by including an additional term on the right of the equation above to yield, for example, in the *V*-band:

$$V - M_V = 5 \log d - 5 + A_V.$$

The absorption due to the interstellar medium varies widely with position in the sky, being most important along directions near the plane of the Galaxy where the concentrations of gas and dust are the highest. Typical determinations of A involve comparisons of the colors of stars of similar type in the same parts of the sky, one nearby (and hence likely to be unaffected by interstellar absorption) and one lying appreciably farther away. In the absence of the availability of such direct comparisons, suitable averages over large parts of the sky are employed. Roughly speaking, interstellar absorption amounts to about 1 magnitude in V for every 1000 pc of distance. The absorption by the interstellar medium is also wavelength dependent in such a way that the more distant the star, the redder it appears; the $(B - V)$ color of a star 1000 pc away would be expected to increase by ~0.3 magnitudes due to this *reddening* effect.

There is one star, the Sun, for which we can directly and precisely measure the flux, not only at visual wavelengths, but, with satellites, at all other wavelengths that do not penetrate to the Earth's surface. Since we also accurately know the distance to the Sun, we may establish the total amount of luminous energy leaving each square meter of surface of the Sun per unit time. In this way, we can establish the absolute magnitude of the Sun in any waveband to good accuracy and use this as a source of comparison for other stars. Moreover, since we know the size of the Sun (and, hence, can compute its total surface area), we can determine the total energy emitted by the Sun each second, that is, its *luminosity*, $L_\odot$. For reference, the luminosity of the Sun is 3.85×10^{26} watts, and its corresponding absolute magnitude is +4.74.

As an example of the use of the Sun as a standard of comparison, if L_* and $L_\odot$ are the total luminosities of a star and the Sun, respectively, then we may write

$$M_{bol}(*) - M_{bol}(\odot) = -2.5 \log (L_* / L_\odot),$$

where the symbols M_{bol} refer to the *absolute bolometric magnitudes* of the star and the Sun. They measure the intrinsic brightness of a star associated with its total flux--that is, the flux integrated (or summed) over all wavelengths.

Now although the bolometric magnitude of the Sun can be quite well established, that for stars is more difficult. And yet this is precisely the quantity that astronomers most want to know insofar as it gives information about the total amount of energy released into space by the star over all wavelengths. However, what can often be conveniently determined is the absolute magnitude of the star in some particular region of the spectrum, say the *V*-band. Since this measures only the amount of radiant energy leaving the star in the visual waveband, it must be corrected in order to account for the radiation being emitted at other (undetected) wavelengths. This correction is called the *bolometric correction*, $BC = M_{bol} - M_V = m_{bol} - m_V$, in as much as it permits us to convert an absolute *V* magnitude into a bolometric magnitude. Bolometric corrections as defined here are negative and vary with the temperature of the star in as much as the spectrum of radiation emitted by a star is a sensitive function of its temperature. As expected, the *BC* is smallest for stars whose temperature (about 6500 K) produces a maximum in the emitted radiation near 550 nm, the peak in the transmission of the *V*-band, and it increases (becomes more negative) for stars that are hotter and cooler than this value. Tabulations of *BC*'s are given in *Allen's Astrophysical Quantities*, *4th Edition*.

With such emendations, we may write for any particular star:

$$M_V + BC = 4.74 - 2.5 \log (L_\star / L_\odot),$$

where we have explicitly inserted the bolometric magnitude of the Sun. Thus, if the absolute *V* magnitude of a star can be found and its bolometric correction is known, its luminosity can be obtained. This is one of the most important parameters for a star for many reasons, not the least of which is that it is needed as a starting value and boundary condition in the construction of stellar model interiors. Of more immediate application, however, is its relationship to the effective temperature and radius of a star.

The luminosity (total energy emitted per unit time) of a star is the product of its radiant flux (energy per unit area per unit time) and its surface area. If the star truly radiated like a blackbody, then theory predicts that its flux would scale as the fourth power of its Kelvin temperature. Although stars do not behave strictly like perfect radiators, we can define a useful temperature indicator, the *effective temperature*, T_{eff}, to be the temperature they would have if their total luminosity was equal to that of an equivalent blackbody. In this way,

$$L = (\text{Flux})\,(\text{Area}) = (\sigma T_{eff}^4)\,(4\pi R^2),$$

where σ is the Stefan-Boltzmann constant, and where we have assumed the star to be a sphere of radius R. If L can be determined from brightness measurements and R is known, then T_{eff} may be calculated. Indeed, if any two of the three quantities L, R, and T_{eff} are given, the third, unknown may be computed. This is another example of a fundamental three-parameter relationship in astronomy (cf. M, m, and d).

The diameter (and hence radius) of a star may be determined from measurements of its angular diameter, providing its distance is known. The basic challenge to measuring the angular size of a star is the fact that it is so small that the blurring of the stellar image due to turbulence in the Earth's atmosphere (an effect called "seeing") effectively swamps the true signal. Various interferometric techniques, including speckle interferometry, as well as lunar occultation methods, have been employed to overcome this problem from the ground. More recently, space-based satellite measurements, free from the influence of the atmosphere, have also been made with the Hubble Space Telescope and Hipparcos. Even so, most of the direct measurements of the sizes of stars beyond our Sun have involved ones that are intrinsically large compared to the Sun or relatively nearby. Stellar radii may also be established for stars in binary systems when the orientation of the orbital planes are such that the two stars eclipse one another as they revolve (see the discussion of double stars below). Table 3 gives some representative angular and linear stellar diameters and the method(s) used to establish the values in each case. We shall come back to the issue of stellar radii and its connection to the luminosity and effective temperature in the next section, but it is noteworthy that, for stars like our Sun ("main sequence" stars), the hotter the star, the larger its radius (cf. Table 3).

STELLAR SPECTRA: THE H-R DIAGRAM

The fact that stars cannot be true blackbody emitters is emphasized by the presence of absorption lines in their spectra. Beginning with the work of J. Fraunhofer in the early decades of the 19th century and continuing today, spectroscopy has provided the primary basis for our understanding of the fundamental characteristics of stars, particularly their temperatures. The use of photographic plates to record the spectra of stars produced by prism (and later grating) instruments attached to ever larger telescopes permitted spectral information for many thousands of stars to be archived and compared. Starting with the work of E.C. Pickering and A. J. Cannon at Harvard, which formed the basis for the *Henry Draper* catalogue, it was recognized that the spectra could be arranged in a one-

parameter sequence based on their appearance. Moreover, changes in the spectra along the sequence were found to be correlated with the color index of the star, and hence, with its temperature. After several refinements, the spectral sequence currently employed by astronomers consists of seven principal classes designated by the letters O, B, A, F, G, K, and M, in order of decreasing temperature. At the cool end of the sequence, one may also now distinguish C (for "carbon") and S stars (the former replacing older R and N classes), depending on the strengths of certain observed molecular bands. Very recent observations of extremely low mass, ultra-cool stars have suggested that the sequence should be extended even further to include objects in classes L and T; approximately one-third of L stars qualify as *brown dwarfs* on the basis of the presence of lithium lines in their spectra. The main stellar spectral classes are, in most cases, further divided into ten sub-classes, numbered 0 to 9, again in order of decreasing temperature; a G0 star is thus hotter than a G5 star.

Classification of stellar spectra is generally done by reference to established standards on what is known as the *Morgan-Keenan* (MK) system. Figure 3 shows intensity tracings of the spectra of some of the stars used to define the MK system, and Table 4 gives a description of the criteria used to determine the *spectral type* along with its associated temperature range. In addition to retaining the Harvard classification scheme, the MK system also codified a second-parameter sequence, the *luminosity class*, based on the strengths of certain spectral lines (e.g., a line of singly ionized strontium, designated Sr II, with wavelength 407.7 nm [4077 Å]), introduced originally in the work of A. Maury at Harvard. Eventually calibrated in terms of the absolute magnitudes of the stars, the MK luminosity classes were given Roman numeral designations as shown in Table 5.

The connection between the number and kinds of absorption lines appearing in a star's spectrum and its temperature may be established using statistical mechanics and atomic theory. The strength of an absorption feature depends on the number of atoms or ions of a given element in a state suitable for absorbing a photon of frequency ν (or wavelength λ) and effecting an upward transition to some state higher in energy by an amount $h\nu$, where h is Planck's constant. If the atoms/ions are assumed to be in thermodynamic equilibrium, then the number density $N_{i,j}$ of absorbers of a given species with ionization i in state j relative to the number density $N_{i,0}$ with ionization i in the ground (lowest) state is proportional to the Boltzmann factor:

$$N_{i,j} / N_{i,0} \propto \exp(-\chi_{i,j} / k\,T).$$

Here, k is Boltzmann's constant and $\chi_{i,j}$ is the excitation energy of the jth state above the ground level. The temperature, T, is the *excitation temperature*.

The number density of absorbers in the ground state with ionization $i + 1$ relative to the number density of those of the same species also in the ground level with ionization i is given by the Saha equation:

$$N_{i+1}\, N_e / N_i \propto T^{3/2} \exp(-\chi_i / k\, T),$$

where χ_i is the ionization energy, N_e is the number density of free electrons, and T is the *ionization temperature*. If the electrons can be considered an ideal gas, then the electron density may be replaced by the electron pressure, $P_e = N_e\, k\, T$, to yield, in logarithmic units:

$$\log N_{i+1} / N_i \propto 5/2 \log T - \chi_i\, (5040 / T) - \log P_e$$

with T in kelvins, χ_i in electron volts, and P_e in dynes/cm^2 ($\approx 10^{-6}$ atm). Applying this equation iteratively when the gas pressure and temperature are known, one may establish the number density of absorbers in any ionization state i relative to the total number density $N = N_1 + N_2 + \ldots + N_i + N_{i+1} + \ldots$, where N_1 is the number density of neutral absorbers, N_2 is the number density of first ionized absorbers, etc. Use of the Boltzmann and Saha equations together thus permits the relative number of absorbers with any ionization and excitation to be computed with respect to the total. The result, as can easily be seen, is dominated by the temperature with pressure effects playing a decidedly subordinate role. To the extent that the rise and fall of the strengths of the spectral lines depends on the number of atoms and ions capable of producing the line and this number is strongly temperature dependent, it is not difficult to see why the spectral sequence is primarily a temperature sequence. Figure 4 shows a plot of line strength versus temperature for several important atoms/ions in stellar atmospheres; the trends revealed in this figure may be easily correlated with the principal criteria used to establish the spectral types in the MK classification system (cf. Table 4). [N.B. In thermal equilibrium, by definition, a gas may be characterized by a single temperature, and there is no longer any difference between the ionization and the excitation temperatures introduced above. This is *not* true when thermodynamic equilibrium does *not* apply, as in regions of stellar atmospheres where the cores of most strong absorption lines are formed or where *emission* lines are produced.]

Although pressure effects enter into the determination of the absorption line strengths in a secondary manner, they are responsible for the characteristics used to establish the luminosity class of the star. Since lower pressures

generally increase the degree of ionization, then, all other things being equal, we would expect an enhancement of the strengths of ionized lines relative to neutral lines in stars with smaller atmospheric pressures. This is the basis upon which the ratios of line strengths involving the Sr II λ4077Å line (e.g., Sr II λ4077/ Fe I λ4045) are used to establish the luminosity class of a star. More generally, however, stars with lower atmospheric pressures tend to have lower surface gravities, and this usually translates to larger radii insofar as $g \propto \mathcal{M} / R^2$. (As we shall see later, the range of stellar masses for normal stars is perhaps of the order of 1000, while that for stellar radii can be 10,000 or more, an effect significantly magnified by the squaring of the radius in the denominator.) Thus, luminosity effects may be correlated with size effects, a result wholly consistent with our earlier relationship showing $L \propto R^2T^4$. This accounts for the terminology invoked to describe the luminosity classes: supergiants, giants, etc. A K0 giant has the same temperature as a K0 supergiant, but the latter is intrinsically brighter (more luminous) than the former because it is larger.

Once the spectral types and luminosity classes have been established for a large number of stars, it is possible to plot luminosity, measured in absolute magnitudes, versus temperature, measured according to spectral type or color. The first such plots were produced independently by H. N. Russell and E. Hertzsprung beginning in about 1913, and are now referred to as *color-magnitude* or *H-R diagrams*. Figure 5 shows such a plot using data from the Hipparcos satellite. What is striking about this diagram is that it is <u>not</u> a scatter plot: stars do not uniformly populate all portions of this plot, but instead occupy certain reasonably well-defined regions. This suggests that the laws of physics/nature do not admit any random combination of luminosity and temperature for real stars, but only certain ones giving rise to the observed distribution.

As can be seen, the majority of stars occupy a strip running diagonally across the plot from very bright, hot O and B stars at the upper left to faint, very cool M stars at the lower right. This is the *main sequence*, which contains stars like our Sun in whose cores hydrogen is being converted into helium by nuclear fusion reactions. Above and to the right of the main sequence there exists another heavily populated region of the H-R diagram consisting of stars with temperatures and colors like those of main sequence G, K, and M stars, but with luminosities more than 10 times greater than their main sequence congeners. These are the *giants* (sometimes called *red giants* because of their color). The great intrinsic brightness of these stars relative to main sequence stars of comparable temperatures

derives from their much larger radii (up to 100 times that of stars in luminosity class V) and surface areas. Such stars represent a later stage in the evolutionary life cycle of a star than the main sequence phase, and they are characterized by core fusion reactions that convert helium to heavier elements like carbon and oxygen.

Arrayed sparsely across the top of the H-R diagram from spectral type O to M are the *supergiants*; as the name implies, these stars owe their large luminosities to their enormous sizes, their radii reaching as much as 1000 or more times the radii of comparable main sequence stars. These stars, while quite conspicuous in the sky because of their tremendous intrinsic brightnesses, are relatively rare, high mass stars that rapidly exhaust their stores of nuclear fuel and remain luminous for only a small fraction of the time that a main sequence star with the same temperature shines. By contrast, at the lower left of the H-R diagram below the main sequence is a small collection of stars with relatively high temperatures but very small luminosities. These stars must be very small in size by comparison to normal stars of the same temperature in order to account for this difference. Such stars are *white dwarfs*, and they represent one endpoint of stellar evolution. Such objects are typically about the size of the Earth, yet contain about a solar mass of material. Consequently, their densities are very high and their interior structures have characteristics in common with those of highly conductive metals. They have no active sources of energy production in their interiors and their store of residual heat is gradually radiated away leaving a burned out stellar cinder, a *black dwarf*.

Once the H-R diagram for stars in the solar neighborhood is established, it may be used as a tool for the assessment of distances to stars too remote for their individual parallaxes to be measured. Applying the H-R diagram in this fashion is at the heart of the method of *spectroscopic parallax*. What is done is to acquire a good spectrum for the star in question and then to classify it completely; that is, determine both its spectral type and luminosity class. With this information, the star can, with reasonable precision, be placed unambiguously on the H-R diagram, and its absolute magnitude established to perhaps 0.5 magnitudes or better. If the apparent magnitude of the star is now measured, the distance modulus can be computed and, in the absence of appreciable interstellar absorption, its distance found. This method works for all stars bright enough to have their spectra measured with good signal-to-noise, and, in practice, it permits us to survey stars out to the edge of our Galaxy (and beyond) with an uncertainty of 20% or less.

BINARY STARS: STELLAR MASSES AND THE MASS-LUMINOSITY RELATION

At least 50% of the stars in the Galaxy are members of binary or multiple star systems. The significance of these systems cannot be over emphasized if for no other reason than they provide astronomers with their best opportunity to determine the masses of stars. And it is the mass that is arguably the most important single parameter describing the star insofar as it controls the star's structure and evolution.

Before describing the means by which stellar masses are determined, we note that binary stars may be classified in various ways, the most common having to do with their mode of discovery. *Visual binaries* are systems that are either close enough to us or widely enough separated that the stars in them can be detected individually at the telescope. This usually demands that the minimum angular separation of the members be larger than a few tenths of an arcsecond on the sky. (Also included in this class are the so-called *astrometric binaries* in which the pair is not actually resolved, but the effect of an unseen companion on the motion of the visible star is manifested as a "wobble" or an oscillation in the path of the star relative to background stars in the same field.) Visual binary systems generally have long periods (>10 years); consequently, to map out the orbit of one star (typically the fainter) relative to its companion usually requires long-term observations of the angular separation and orientation of the two stars (see Figure 6). For much of the history of the study of such binaries this meant painstaking observations using long focal length refracting telescopes. Within the last twenty-five years, special interferometric techniques have enabled astronomers to detect and monitor visual binaries with separations of the order of a few tens of milli-arcseconds with unprecedented accuracy. This has dramatically added to our understanding of these systems and to our knowledge of the masses of the stars in them.

Stars too far away or too close together to be resolved at the telescope may be detected spectroscopically from the variations in their radial velocities as revealed by the periodic shifts in the wavelength of their spectral lines according to the Doppler principle (Figure 7). Such systems are referred to as *spectroscopic binaries*. In some of these cases, the orbital planes of the stars make sufficiently small angles with the line of sight to the system that the two components eclipse one another. For such *eclipsing binaries*, the change in the brightness of the system throughout an orbital period (the "light curve") may be monitored, and, when coupled with velocity information

from the spectra, used to establish the radii of the two stars and the ratio of their surface brightness (Figure 8). There exists at least one other type of double star system that may be distinguished observationally, the *spectrum binaries*. These are distant stars whose separation is too wide to permit easy observation of their velocity changes, but whose duplicity is revealed by the composite nature of their spectra: two different spectra superimposed in a single image.

Although the classification of binary stars on the basis of their means of detection is convenient, it is in no way fundamental or particularly illuminating in terms of the properties or characteristics of these systems or the stars contained in them except in the most general of ways. There are clear overlaps in the classes (all eclipsing binaries are at least potentially spectroscopic binaries), and each is fraught with selection effects, although in different ways (e.g., distance is an important selection effect for the discovery of visual binaries, but not so much so for spectroscopic binaries). Alternative binary classification schemes have been proposed emphasizing either the relative luminosities of the stars, their masses and radii, or some combination of these parameters, and while physically more meaningful, they are still less frequently used in popular descriptions of binary stars.

Stellar masses may be determined for binary star systems using Newtonian mechanics. In an isolated binary system containing two stars of mass $\mathcal{M}_1$ and $\mathcal{M}_2$ orbiting their mutual center-of-mass at distances r_1 and r_2, the gravitational force of attraction between the masses provides the force needed to keep them in orbit. The general shapes of the orbits of the stars may be shown to be elliptical with the center-of-mass occupying one focus of each ellipse (cf. Figure 9). Since the equation for the center-of-mass ($\mathcal{M}_1 r_1 = \mathcal{M}_2 r_2$) holds for all times t, it must be the case that $\mathcal{M}_1 a_1 = \mathcal{M}_2 a_2$, where $a_{1,2}$ are the semi-major axes of the orbits of $\mathcal{M}_1$ and $\mathcal{M}_2$. The mass ratio thus becomes:

$$\mathcal{M}_1 / \mathcal{M}_2 = a_2 / a_1.$$

Differentiating the equation for a fixed center-of-mass also permits us to write the mass ratio in terms of the orbital speeds of the stars:

$$\mathcal{M}_1 / \mathcal{M}_2 = v_2 / v_1.$$

The sum of the masses may be obtained by applying conservation of angular momentum while invoking the properties of ellipses to obtain:

$$\mathcal{M}_1 + \mathcal{M}_2 = 4 \pi^2 a^3 / G \mathrm{P}^2,$$

where P is the orbital period of either star and $a = a_1 + a_2$. Thus, the equation for the sum of the masses may be combined with that for the ratio of the masses to give the individual stellar masses. Since the periods of most binaries can be established with considerable accuracy, the quality of the mass determinations depends primarily on the accuracy with which the semi-major axes can be established. Roughly speaking, the fractional uncertainty in the total system mass is about three times that of the semi-major axis.

The process of determining the masses as outlined above is complicated by the fact that most orbits are not conveniently oriented with their planes perpendicular to the line of sight, but are typically inclined to it by $(90° - i)$, where i is the inclination angle. (The angle i is defined such that $i = 90°$ if the plane of the orbit contains the line of sight.) Taking account of the orientation of the orbits is a tricky business, but one which can be accomplished for visual binaries. By doing so, the angle a'' subtended by the true relative semi-major axis for such systems can be determined, and then converted into the semi-major axis a in physical units if the distance is known: $a'' = a / d$, with a'' in radian measure and the units of a and d the same. Alternatively, $a'' = p\, a$, with a'' and p, the parallax, in arcseconds, and a in parsecs.

For a spectroscopic binary with both spectra measurable, only the quantity $a \sin i$ can be determined from the observed amplitude of the radial velocity variation. However, if the system is also an eclipsing one, then a separate evaluation of $\sin i$ may be made from the shape of the light curve. Otherwise, the mass sum remains uncertain by a factor of $(\sin i)^3$, and therefore so too do the individual masses. Occasionally, statistical arguments are used to establish an average value for the quantity $\sin^3 i$ and, hence, to recover approximate values for the separate stellar masses. For example, if the inclination of the orbital planes of binary stars are distributed at random in space, then it is possible to show that $\langle(\sin i)^3\rangle = 0.59$; correction for selection effects having to do with the probability of discovering a spectroscopic binary raises the value of $\langle(\sin i)^3\rangle$ to about 0.67.

If, in a spectroscopic binary, only one star is visible, then the amount of information accessible to us concerning the system mass is even further reduced. In this case, the best that can be done is to determine what is called the *mass function*,

$$f(\mathcal{M}_1, \mathcal{M}_2) = \mathcal{M}_2^3 \sin^3 i / (\mathcal{M}_1 + \mathcal{M}_2)^2.$$

In most cases, the mass function is useful for statistical purposes, or to estimate the mass of one star, assuming the mass of the other has been established by some indirect means.

If one plots the masses of main sequence stars versus their luminosities ($= 4 \pi R^2 \sigma T_{eff}^4$), there results a monotonic relation between these two fundamental stellar parameters, viz., the larger the mass, the greater the luminosity (cf. Figure 10). The origin of this relationship may be understood in terms of the physical process that powers main sequence stars: the fusion of hydrogen in their cores which produces helium and releases energy according to Einstein's famous equation $E = m c^2$. Since stars are composed primarily of hydrogen, the greater the stellar mass, the more fuel is available to power the star and the greater the luminosity. Moreover, the greater the mass, the greater the gravitational compression of the material in the core; this yields higher core temperatures, increased reaction rates, and again, higher luminosities. Together, these factors produce luminosities that scale as the mass of the star to the power 2 to 4 over the entire range of observed stellar mass. It is worth noting that the mass-luminosity relation does not hold for evolved stars like red giants or white dwarfs.

CONCLUSION

The foregoing discussion has, because of limits of space, touched upon only the most basic characteristics of stars: masses, radii, temperatures, and luminosities. There exist numerous other properties of stars that are important for determining their structure, evolution, and dynamics, including their composition, density, rotation, magnetic field strength, mass loss rate, space velocity, etc. In each case, specialized observational and analytical techniques are employed to extract needed information from the star's light, in particular from its spectrum. For example, stellar absorption lines are broadened by rotation due to the Doppler effect; studying the distinctive "dish"-shaped line profiles produced by rapidly rotating stars permits an assessment to be made of their speeds of rotation. Similarly, by studying the Zeeman splitting of spectral lines due to the presence of magnetic fields in stars, information may be gleaned about the strength and orientation of these fields over a broad range of temperature. Table 6 briefly summarizes some additional properties of stars that may be of interest to engineers and other non-specialists who may at some point be involved in astronomical research and development. For more detail, the reader is encouraged to consult some of the references given below.

REFERENCES

Cox, A. N., Ed., *Allen's Astrophysical Quantities, 4th Edition*; AIP Press/Springer-Verlag: New York, NY, 2000.

Bohm-Vitense, E., *Introduction to Stellar Astrophysics: Vol. I – Basic Stellar Observations and Data*; Cambridge University Press: Cambridge, 1989.

Carroll, B. W.; Ostlie, D. A., *An Introduction to Modern Astrophysics*; Addison-Wesley: Reading, MA, 1996.

Harwit, M., *Astrophysical Concepts, 3rd Edition*; Springer-Verlag: New York, NY, 1998.

Zeilik, M.; Gregory, S. A., *Introductory Astronomy and Astrophysics, 4th Edition*; Saunder's College Publishers: Fort Worth, TX, 1998.

Table 1. Some important characteristics of the 25 brightest stars. For binary and multiple systems, the integrated apparent magnitude is given; all other properties are for the brightest component only.

Star	RA (hh mm)	Dec (dd mm)	Apparent Magnitude	Distance[§] (pc)	Spectral Type	Absolute[‡] Magnitude
α Canis Majoris (Sirius)	6 45	-16 42	-1.4[*]	2.6	A1 V	+1.5
α Carinae (Canopus)	6 24	-52 42	-0.6	96	F0 Ib	-5.5
α Centauri (Rigil Kent)	14 40	-60 50	-0.3[*]	1.3	G2 V	+4.4
α Bootis (Arcturus)	14 16	+19 11	-0.1	11	K2 III	-0.3
α Lyrae (Vega)	18 37	+38 47	0.0	7.8	A0 V	+0.5
α Aurigae (Capella)	5 17	+46 00	0.0[*]	13	M1 III	-0.6
β Orionis (Rigel)	5 15	-8 12	0.1[*]	237	B8 Ia	-6.8
α Canis Minoris (Procyon)	7 39	+5 14	0.3[*]	3.5	F5 IV-V	+2.7
α Eridani (Achernar)	1 38	-57 14	0.5	44	B3 V	-2.7
β Centauri (Hadar)	14 04	-60 22	0.6[*]	161	B1 III	-4.1
α Aquilae (Altair)	19 51	+8 52	0.8	5.1	A7 IV-V	+2.2
α Orionis (Betelgeuse)	5 55	+7 24	0.5[†]	131	M2 Ib	-5.1
α Tauri (Aldebaran)	4 36	+16 31	0.9[*]	20	K5 III	-0.6
α Crucis (Acrux)	12 27	-63 04	0.8[*]	98	B0.5 IV	-4.2
α Virginis (Spica)	13 25	-11 10	1.0[†]	80	B1 V	-3.6
α Scorpii (Antares)	16 29	-26 26	1.1[*†]	185	M1 Ib	-5.2
β Geminorum (Pollux)	7 45	+28 02	1.2	10	K0 III	+1.2

α Piscis Austrini (Formalhaut)	22 58	-29 37	1.2	8	A3 V	+1.7
α Cygni (Deneb)	20 41	+45 17	1.3	990	A2 Ia	-8.7
β Crucis (Mimosa)	12 48	-59 41	1.3	108	B0.5 III	-3.9
α Leonis (Regulus)	10 08	+11 58	1.4*	24	B7 V	-0.5
ε Canis Majoris (Adhara)	6 59	-28 58	1.5	132	B2 II	-4.1
α Geminorum (Caster)	7 35	+31 53	1.6	16	A2 V	+0.6
γ Crucis (Gacrux)	12 31	-57 07	1.6	27	M4 III	-0.6
λ Scorpii (Shaula)	17 34	-37 06	1.6	216	B1.5 IV	-5.1

§Distance calculated from parallax measurements made by Hipparcos.

‡Absolute magnitude calculated using $M = m + 5 - 5 \log d$.

*Multiple star system.

†Variable star.

Table 2. Characteristics of several common photometric magnitude systems.*

System	Band	Central Wavelength (nm)	Bandwidth† (nm)
Johnson-Morgan[1]	U	360	70
	B	440	100
	V	550	90
	R	700	220
	I	880	240
Infrared	J	1250	260
	H	1650	290
	K	2200	410
	L	3500	570
	M	4800	450
Geneva[2]	B_1	402	17
	B_2	448	16.5
	V_1	541	20
	G	581	21
Strömgren	u	350	38
	v	410	20
	b	470	20
	y	555	20
	Hβ	486	15/3[3]

*Filter characteristics for other photometric systems not included here, like the Walraven system, the Vilnius seven-color system, the DDO five-color system, etc., may be found in *Allen's Astrophysical Quantities*, *4th Edition,* p. 386.

†The filter full width at half maximum transmission.

[1]The Cousins or "Cape" system is similar to the Johnson-Morgan system in using the standard UBV bandpasses, but its R and I bands have mean wavelengths at 670 nm and 810 nm, respectively.

[2]The Geneva system employs the standard UBV filters plus those listed in the table.

[3]Two Hβ filters, a narrow and a wide one, with the bandpasses listed, are commonly employed.

Table 3. Some characteristic stellar radii for bright stars

Star	Spectral* Type	Angular Diameter† (milliarcsec)	Radius‡ ($R_\odot$§)	Method
ζ Oph	O9.5 V	0.51 ± 0.05	7.68	Intensity Interferometry
EM Car A	O9.5 V		9.34	Eclipsing Binary
EM Car B	O9.5 V		8.33	Eclipsing Binary
CW Cep A	B0.4 V		5.69	Eclipsing Binary
CW Cep B	B0.7 V		5.18	Eclipsing Binary
α Pav	B2.5 V	0.80 ± 0.05	4.82	Intensity Interferometry
U Oph A	B5 V		3.44	Eclipsing Binary
U Oph B	B5 V		3.01	Eclipsing Binary
α Leo	B7 V	1.37 ± 0.06	3.49	Intensity Interferometry
α Lyr	A0 V	3.24 ± 0.07	2.70	Intensity Interferometry
PV Cas A,B	A0 V		2.26	Eclipsing Binary
α CMa A	A1 V	5.89 ± 0.16	1.68	Intensity Interferometry; Visual Binary
α PsA	A3 V	2.10 ± 0.14	1.73	Intensity Interferometry
α Aql	A7 IV-V	2.98 ± 0.14	1.64	Intensity Interferometry
RS Cha A,B	A8 V		2.24	Eclipsing Binary
γ Vir A,B	F0 V		1.35	Visual Binary
PV Pup A,B	F1 V		1.52	Eclipsing Binary
α CMi A	F5 IV-V		2.06	Visual Binary
UX Men A,B	F8 V		1.31	Eclipsing Binary

η Cas A	G0 V		0.98	Visual Binary
EW Ori A	G0 V		1.14	Eclipsing Binary
EW Ori B	G2 V		1.09	Eclipsing Binary
α Cen A	G2 V		1.27	Visual Binary
BH Vir B	G5 V		1.14	Eclipsing Binary
ξ Boo A	G8 V		0.77	Visual Binary
FL Lyr B	G9 V		0.96	Eclipsing Binary
ζ Her B	K0 V		0.79	Visual Binary
HS Aur B	K0 V		0.87	Eclipsing Binary
CG Cyg B	K4 V		0.84	Eclipsing Binary
RT And B	K4 V		0.90	Eclipsing Binary
η Cas B	M0 V		0.59	Visual Binary
CM Dra A,B	M4 V		0.24	Eclipsing Binary
γ Ori	B2 III	0.72 ± 0.04	5.76	Intensity Interferometry
γ Crv	B8 III	0.75 ± 0.06	4.06	Intensity Interferometry
α Oph	A5 III	1.63 ± 0.13	2.50	Intensity Interferometry
ξ^2 Sgr	K1 III	3.80	37.1	Lunar Occultation
ν Cap	M2 III	4.72	26.6	Lunar Occultation
μ Gem	M3 III	13.65	73.2	Lunar Occultation
ψ Vir	M3 III	5.86	29.9	Lunar Occultation
RZ Ari	M6 III	10.18	78.0	Lunar Occultation
ε Ori	B0.6 Ia	0.69 ± 0.04	18.55	Intensity Interferometry

η CMa	B5 Ia	0.75 ± 0.06	78.86	Intensity Interferometry
β Ori	B8 Ia	2.55 ± 0.05	64.81	Intensity Interferometry
α Car	F0 Ib-II	6.6 ± 0.8	67.87	Intensity Interferometry
δ CMa	F8 Ia	3.60 ± 0.50	212.2	Intensity Interferometry

*The table is arranged according to decreasing temperature within each luminosity class: V = main sequence stars; III = giant stars; and Ia,b = supergiant stars.

†True angular diameter corrected for non-uniform brightness across the stellar disk (i.e., *limb darkening*).

‡For stars with measured angular diameters, θ, and known distances (or parallaxes, p), the radius, $R = (107.2527)\ \theta / p$; the uncertainties in R mirror those in θ and are generally ≤10%. For eclipsing binaries, R is determined using the technique illustrated in Figure 8; the uncertainties in R for this class of stars are typically ≤2%. For visual binaries, R is found from the distances and surface fluxes, and, with the exception of η Cas B whose fractional uncertainty is 0.3, the values are accurate to ~10% or less.

§ $\mathbf{R}_{\odot}$ = the radius of the sun, 6.96×10^8 meters.

Table 4. Classification of stellar spectra.

Spectral Type	Temperature (K)	(B - V)*	Spectral Criteria†
O5	50,000	-0.33	Strong He II lines; He I lines weak but increasing in strength from O5 to O9. Hydrogen Balmer lines relatively weak. Lines of highly ionized atoms (Si IV, N III, O III, C III) present.
B0	25,000	-0.30	He II lines absent; He I lines dominate, reaching peak intensity at B2. Hydrogen lines increasing in strength from B0 to B9. Si III and O III lines prominent.
A0	11,000	-0.02	He I absent; hydrogen Balmer lines reach maximum strength at A0. Lines of ionized metals (Fe II, Mg II, Si II) achieve maximum strength near A5. Ca II lines are weak, while lines of neutral metals are just appearing.
F0	7,600	+0.30	Balmer lines weakening rapidly, while Ca II lines strengthening. Neutral metal lines (Fe I, Cr I) gain in strength relative to corresponding singly ionized species.
G0	6,000	+0.58	Hydrogen lines very weak; Ca II lines reach maximum strength near G2. Neutral metals (Fe I, Mn I, Ca I) are strong. Molecular CH band becomes prominent.
K0	5,100	+0.81	Hydrogen lines nearly absent; neutral atomic lines strong. Molecular TiO bands appear in late K spectra.
M0	3,600	+1.40	Neutral metal lines (e.g., Ca I) very strong; molecular bands prominent, with TiO dominant by M5; VO bands beginning to appear.
C	3,000	**	Strong CN, CO, and C_2 bands; TiO absent. Neutral metals as in K and M types.

S	3,000	**	Strong ZrO, YO, LaO bands; neutral metals as in K and M types.
L0	2,000	+4.5	Metal hydrides (e.g. FeH, CrH) strong; VO reaches maximum at L0. Alkali metal absorption (K I, Cs I, Rb I) strengthens towards L8, while hydrides weaken.
T	1,000	***	Metal oxides weak; FeH strong, while CrH weakens. Cs I prominent, and H_2O present. Strong methane bands appear.

*Color indices are for main sequence stars.

†In designating the various absorbers, standard spectroscopic notation has been adopted wherein neutral species are signified by Roman numeral "I", singly ionized species by "II", doubly ionized species by "III", and so on.

**C and S stars are giants with (B – V) colors ranging from about +0.9 to around +1.6.

***T dwarfs are so cool and faint that they cannot be observed visually, and, hence, have no measured visual colors. Instead, an infrared color index may be defined for these stars, yielding values $\geq$5.5.

Table 5. Morgan-Keenan Luminosity Classes*

Class†	Name
I	Supergiants
II	Bright Giants
III	Giants
IV	Subgiants
V	Dwarfs[1]

*The assessment of luminosity is based on the appearance of certain pairs of lines in the blue portion of the spectrum as compared to standard stars. For example, in the spectral range B0 to B3, the ratio of lines of singly ionized nitrogen at 399.5 nm to those of singly ionized helium at 400.9 nm are used, while between A3 and F0, the ratio of singly ionized magnesium lines at 441.6 nm and 448.1 nm is employed.

†Each class may be divided into subclasses marked *a*, *ab*, and *b*, for example, Iab. For a given spectral type, luminosity decreases along the sequence *a, ab, b*. Some authors include a sixth luminosity class, VI, which includes so-called *subdwarf* stars.

[1]These are main sequence stars.

Table 6. Some additional properties of stars

A. Element Abundances*

Element	At. No.	Abundance	Element	At. No.	Abundance
Hydrogen (H)	1	12.00	Calcium (Ca)	20	6.36
Helium (He)	2	10.99	Sodium (Na)	11	6.33
Oxygen (O)	8	8.93	Nickel (Ni)	28	6.25
Carbon (C)	6	8.56	Chromium (Cr)	24	5.67
Neon (Ne)	10	8.09	Chlorine (Cl)	17	5.50
Nitrogen (N)	7	8.05	Phosphorus (P)	15	5.45
Magnesium (Mg)	12	7.58	Manganese (Mn)	25	5.39
Silicon (Si)	14	7.55	Potassium (K)	19	5.12
Iron (Fe)	26	7.54	Titanium (Ti)	22	4.99
Sulfur (S)	16	7.21	Cobalt (Co)	27	4.92
Argon (Ar)	18	6.56	Zinc (Zn)	30	4.60
Aluminum (Al)	13	6.47	Fluorine (F)	9	4.56
			Copper (Cu)	29	4.21

*Logarithmic abundances for the 25 most abundant elements in the Sun's photosphere, normalized to log(H) = 12.00. These abundances are considered to be the standard "cosmic" abundances, and are characteristic of Population I stars in the Galaxy. In older, Population II stars, the overall abundance of elements heavier than helium, the so-called *metals*, may be lower by two or even three orders of magnitude. In all but a few cases, the abundances derived from the solar photosphere agree to within the uncertainties of measurement with the abundances determined from the analyses of samples of undifferentiated meteoritic material recovered on Earth.

B. Rotational Velocities*

Spectral Type	$< v_e \sin i >$† (km/s)		$< v_e >$‡ (km/s)	
	III	V	III	V
O5		140		
B0	75	160	95	200
B5	95	180	120	230
A0	110	150	140	190
A5	125	115	160	150
F0	100	78	130	100
F5	45	22	60	30
G0§	15	3	20	4
K,M	<10	1	<12	1

*High rotational velocities typically occur only in stars hotter than the sun, viz. O, B, A, and F stars, not among the cooler spectral types. For a given spectral type, there is a noticeable difference between the rotational speeds for giant stars (III) and main sequence stars (V), with the former having smaller values up to about spectral type A5 and larger ones thereafter.

†Mean *apparent* equatorial rotational velocity observed for inclination angle i of the axis of rotation with respect to the line-of-sight to the star.

‡Mean equatorial rotational velocity assuming a random distribution of inclination angles i with $< \sin i > = \pi / 4$.

§For comparison, the mean equatorial rotation speed of the Sun (G2 V) is 1.98 km/s.

C. Magnetic Fields

Star Class	Magnetic Field* (gauss)
Normal Stars†	
O – B	≤ 500
A - M‡	≤ 200
Peculiar Stars (Ap-Bp)§	
Hg-Mn	≤ 200
Si, Si-Cr-Eu	~200 – 20,000
Am	≤ 150
He weak	~200 – 7000
He strong	≥ 1000

*Values generally represent the longitudinal (effective) magnetic field, irrespective of its polarity, based on measurements of circular polarization in spectral lines. For stars with low rotational speeds ($v \sin i \leq 30$ km/s) and large fields ($\geq$ 1000 G), integrated surface magnetic field strengths may be obtained from Zeeman split lines; in such cases, the surface fields are 2-3 times stronger than the largest longitudinal fields. In the table, values prefaced with "≤" represent upper-limits, and, in the light of the typical errors of measurement, may be consistent with zero field.

†This includes stars of all luminosity classes, supergiants through dwarfs (main sequence stars), but excludes stars in X-ray--emitting binary systems.

‡Magnetic fields in the range 1000--3000 G have been observed in some cool (> G5) main sequence stars by means of Zeeman broadening in certain spectral lines. These observations suggest the existence of large magnetic plages that may cover from 30% up to ~80% of the stars' surfaces. For reference, the maximum mean magnetic field of the Sun is about one gauss, while that in sunspot umbrae can reach several thousand gauss.

§These are typically stars of spectral type A and B that exhibit abundance patterns that differ significantly from that of the Sun and most other "normal" stars (cf. Table 6A). Subclasses within the Ap-Bp group are usually designated in terms of the elements showing the greatest departure (commonly over abundances) from the standard abundance distribution. In *metallic line A* stars (Am's), the lines of the heavy elements are all too strong in comparison with the hydrogen lines, while the lines of singly ionized calcium are too weak. In most of the stars with substantial magnetic fields, the field strengths are found to very in a nearly sinusoidal manner, the period of which is almost

certainly the rotation period of the star. Most stars have periods in the range of 1--10 days.

FIGURE CAPTIONS

Fig. 1--Establishing the distance to a star by the method of trigonometric parallax. (After F. H. Shu, *The Physical Universe: An Introduction to Astronomy* (University Science Books: Mill Valley, CA), 1982.) Measurement of the angles θ' and θ" are made using images of the sky containing the nearby star from opposite sides of the Earth's orbit. From the geometry of the figure, $\theta' + \theta'' = 2p$, where p is the *parallax angle*. For large d, the angle p is small, yielding $\tan p \sim p = 1 \text{ AU} / d$, with p in radians and d in AU.

Fig. 2--Earth's atmospheric transparency to electromagnetic radiation of wavelength 8 (in meters) and frequency ν (in hertz). (Reprinted with permission from J. Binney and M. Merrifield, *Galactic Astronomy* (Princeton University Press: Princeton, NJ), 1998.) The solid lines locate the height at which the intensity of incident radiation is reduced by $1/e$. "Windows" in the atmosphere exist in the optical, throughout most of the radio, and in selected portions of the infrared regions of the spectrum. Additional IR observations are facilitated by making measurements from mountaintops and via instrumentation borne aloft in aircraft, balloons, rockets, and orbiting spacecraft. The atmosphere is opaque to high-energy radiation (UV, X-rays, and γ-rays), which can be detected only with the use of instruments flown in balloon and rocket experiments or in satellites.

Fig. 3--Sequence of digital spectra of main sequence (luminosity class V) stars. (Images courtesy of D. O. Gray, Appalachian State University; see http://nedwww.ipac.caltech.edu/level5/Gray/Gray_contents.html). CCD images of classified spectra of stars from O9 to M4.5 (a – e) are shown with critical features identified. In panel (f), the luminosity classes Ia,b (supergiants) and II (bright giants) at A0 ($T \sim 10{,}000$ K) have been included to demonstrate variations attributable to pressure, as opposed to temperature, effects. Note particularly the gradual weakening of the features associated with ionized species and the steady broadening of the hydrogen lines as the luminosity declines and the mean atmospheric pressure rises.

Fig. 4--Number of absorbers in ionization state i with excitation j, N(i,j), relative to the total number N of such species for selected atoms and ions of importance in stellar spectral classification. (After A. Unsöld and B. Baschek, *The New Cosmos*, 3rd edition (Springer-Verlag: New York), 1985.) The plot reflects the populations of absorbers in

excitation states responsible for the production of the Balmer lines in neutral hydrogen (H I), the 4026 Å and 4471 Å lines in neutral helium (He I), the 4686 Å line in singly ionized helium (He II), the 4226 Å line in neutral calcium (Ca I), and the 3934 Å and 3968 Å lines (K and H, respectively) in singly ionized calcium (Ca II). Solar abundances and a representative mean value of 100 dynes/cm^2 for the electron pressure has been adopted in these calculations.

Fig. 5--H-R diagram based on Hipparcos data. (From the Hipparcos website; see http://astro.estec.esa.nl/Hipparcos/hipparcos.html.) This plot includes absolute V-magnitudes and $(B - V)$ colors for 41705 single stars whose distances are known to better than 20% and whose colors are accurate to within 0.05 magnitudes. The color bar indicates the number of stars in a cell of dimension 0.01 magnitudes in $(B - V)$ by 0.05 magnitudes in M_V. The main sequence and giant branch are clearly delineated in this figure, and a few nearby white dwarfs may also be identified. For reference, the $(B - V, M_V)$ coordinates of the Sun on this plot are (+0.65, +4.82).

Fig. 6--Apparent relative orbit of a visual binary. Micrometer measurements yield the separation in arcseconds and the position angle in degrees reckoned increasingly positive from the northpoint in an easterly direction. The data trace the projection of the true orbit of the fainter companion relative to the brighter (and typically more massive) primary on the sky; it is for this reason that the primary does not necessarily lie near one focus of the apparent ellipse as required by Newtonian theory.

Fig. 7--Radial velocity curve for the double-lined spectroscopic binary HR 7955 (Data courtesy of Dr. R. F. Griffin, Cambridge Observatories). The period of the system is 523.4 days, and the center-of-mass velocity is 32.8 km/s towards us. (Negative radial velocities imply motion of the source towards the observer; positive values indicate motion away.) Phase point zero is taken to be the time when the two stars are as close together as possible. Open circles represent measurements for the primary (more massive) star; crosses are measurements for the secondary. Since the amplitudes of the velocity curves relative to the center-of-mass motion are nearly equal, the stars have approximately the same mass. The eccentricity of the system is quite high, 0.55, accounting, in the main, for the distortion of the curves from simple sinusoids expected for circular orbits.

Fig. 8--Schematic light curve for an eclipsing binary star. In this model, the stars are assumed to be spherical in shape and the orbits are taken to be circular; the effects of limb darkening are ignored. The vertical axis displays the total system luminosity, while the horizontal axis shows elapsed time measured as a fraction of the total period, reckoned from the midpoint of the primary (deepest) eclipse. The period, P, of the system is 7.2 days, the mean separation, a, between the stars is 0.1 AU, the ratio of the stellar radii is 7-to-1, and the inclination angle, i, is 90°. The primary eclipse occurs when the smaller, hotter star is covered by its larger, cooler companion. If the overall duration of the eclipse, T, and the time of the duration of the central phase, t, are known, then the stellar radii may be found from $R_{1,2} = (v/4)\,(T \pm t) = (\pi\, a / 2\, P)\,(T \pm t)$, where R_1 applies to the larger star and R_2 to the smaller. The relative velocity of one star with respect to the other is represented by v.

Fig. 9--Geometry of a binary star system. Each star's orbit is an ellipse, with the center-of-mass, C, of the system at one focus of the ellipse. The center-of-mass is defined by the condition that $M_1\, r_1 = M_2\, r_2$. The orbital period of each star is the same, and the semi-major axis of the relative orbit of one star about the other is just the sum of the semi-major axes of the orbits of the individual stars with respect to the center-of-mass: $a = a_1 + a_2$.

Fig. 10--Mass-luminosity relation for main sequence stars. (Data courtesy of Dr. Guillermo Torres, Smithsonian Astrophysical Observatory.) A nearly linear relation between log (L) and log (M) is seen ranging over more than eight decades in L and two decades in M.

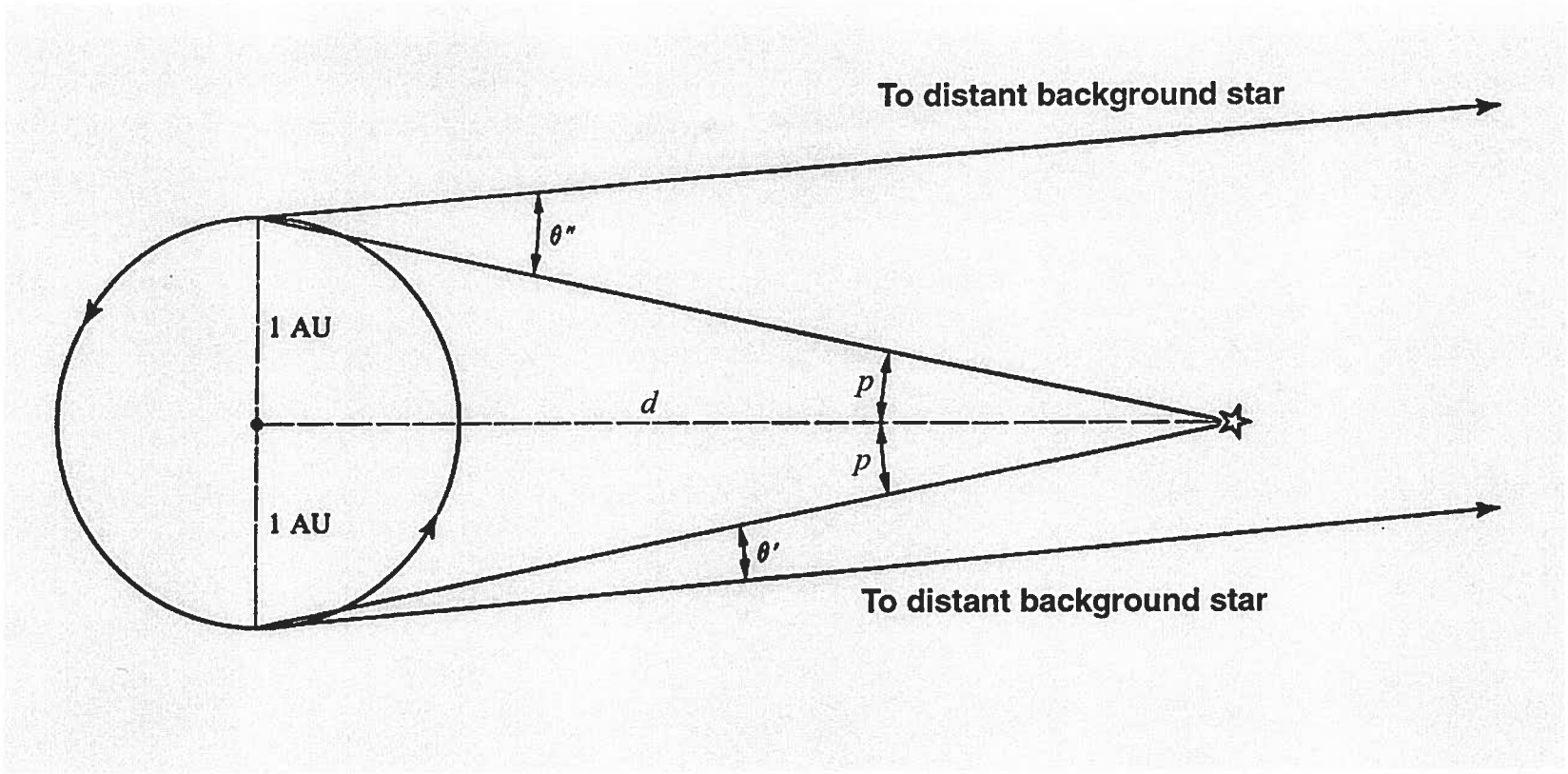
To distant background star
θ″
1 AU
d
p
p
1 AU
θ′
To distant background star

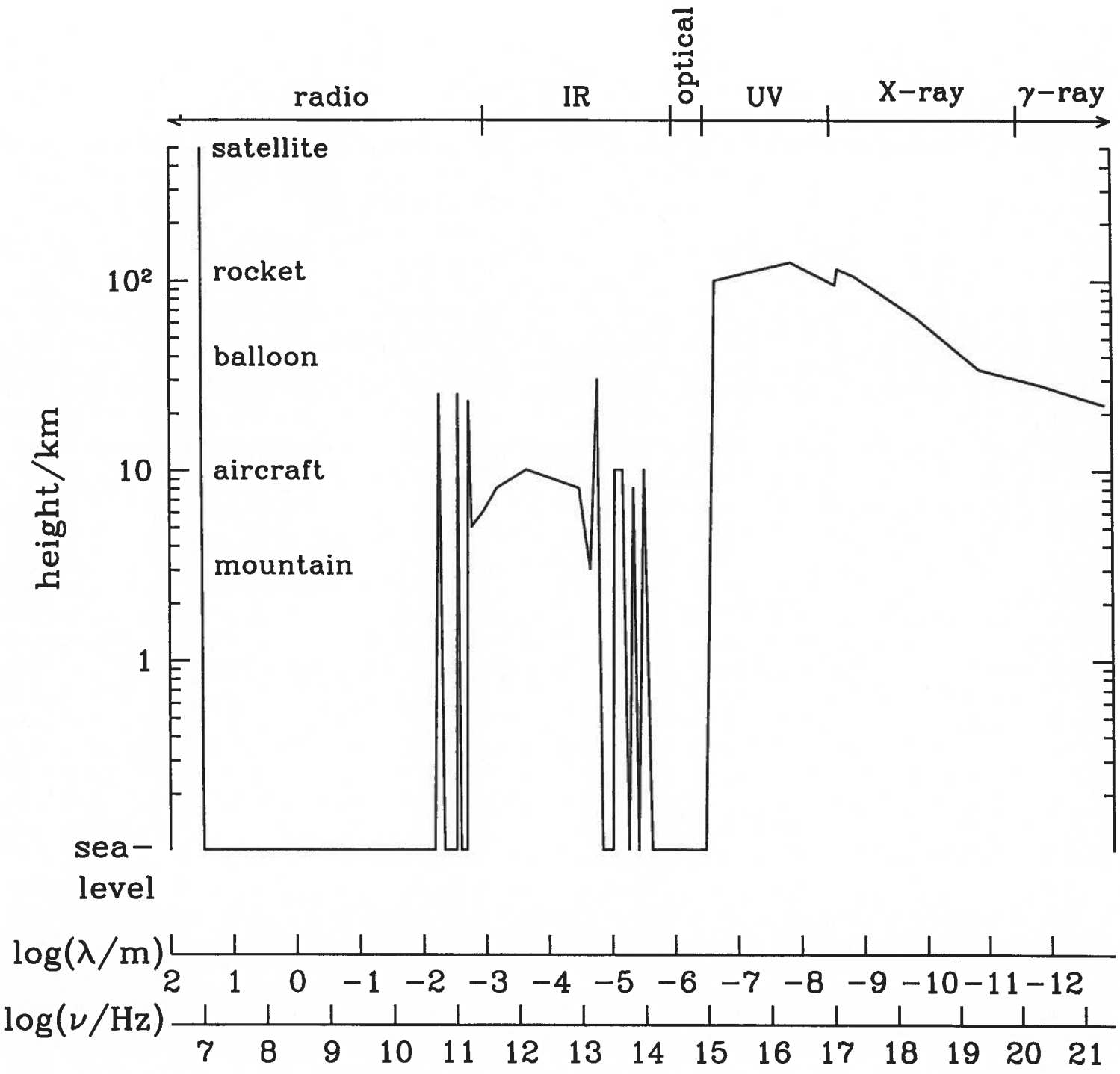
radio
IR
optical
UV
X-ray
γ-ray
satellite
rocket
balloon
aircraft
mountain
sea-level
height/km
10²
10
1
log(λ/m)
2 1 0 −1 −2 −3 −4 −5 −6 −7 −8 −9 −10 −11 −12
log(ν/Hz)
7 8 9 10 11 12 13 14 15 16 17 18 19 20 21

Main Sequence O9 – B5

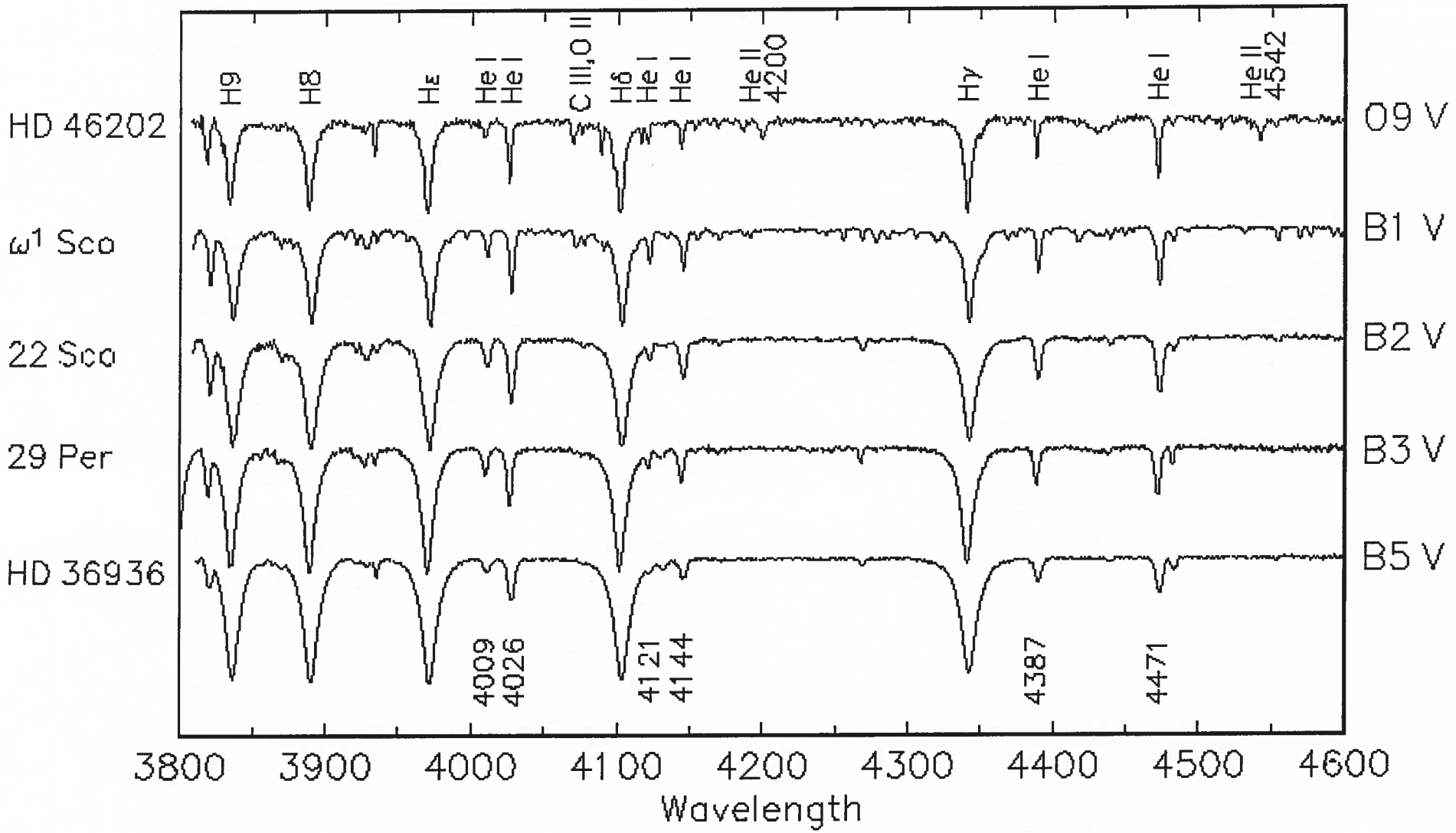

Main Sequence B5 – A5

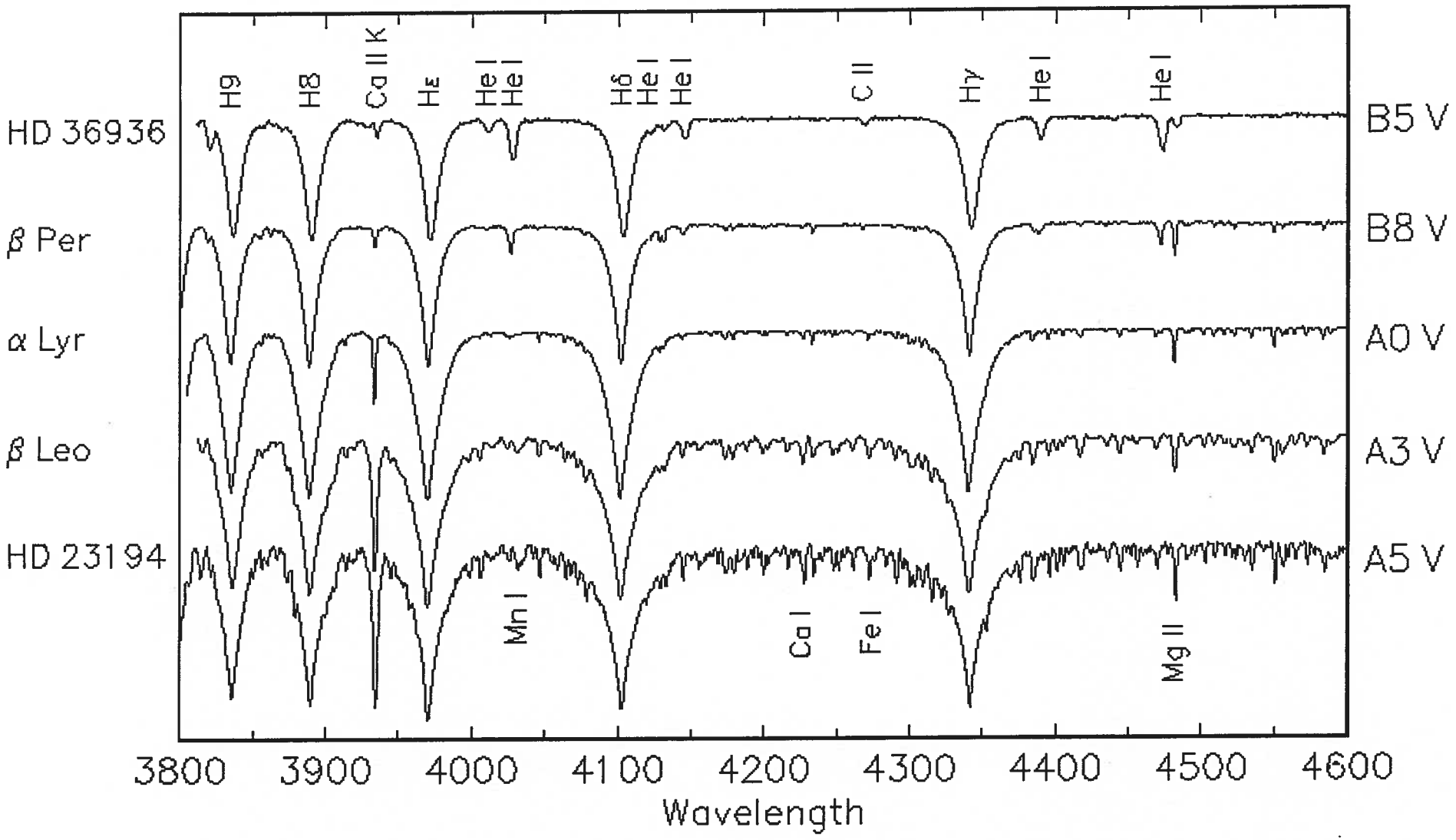

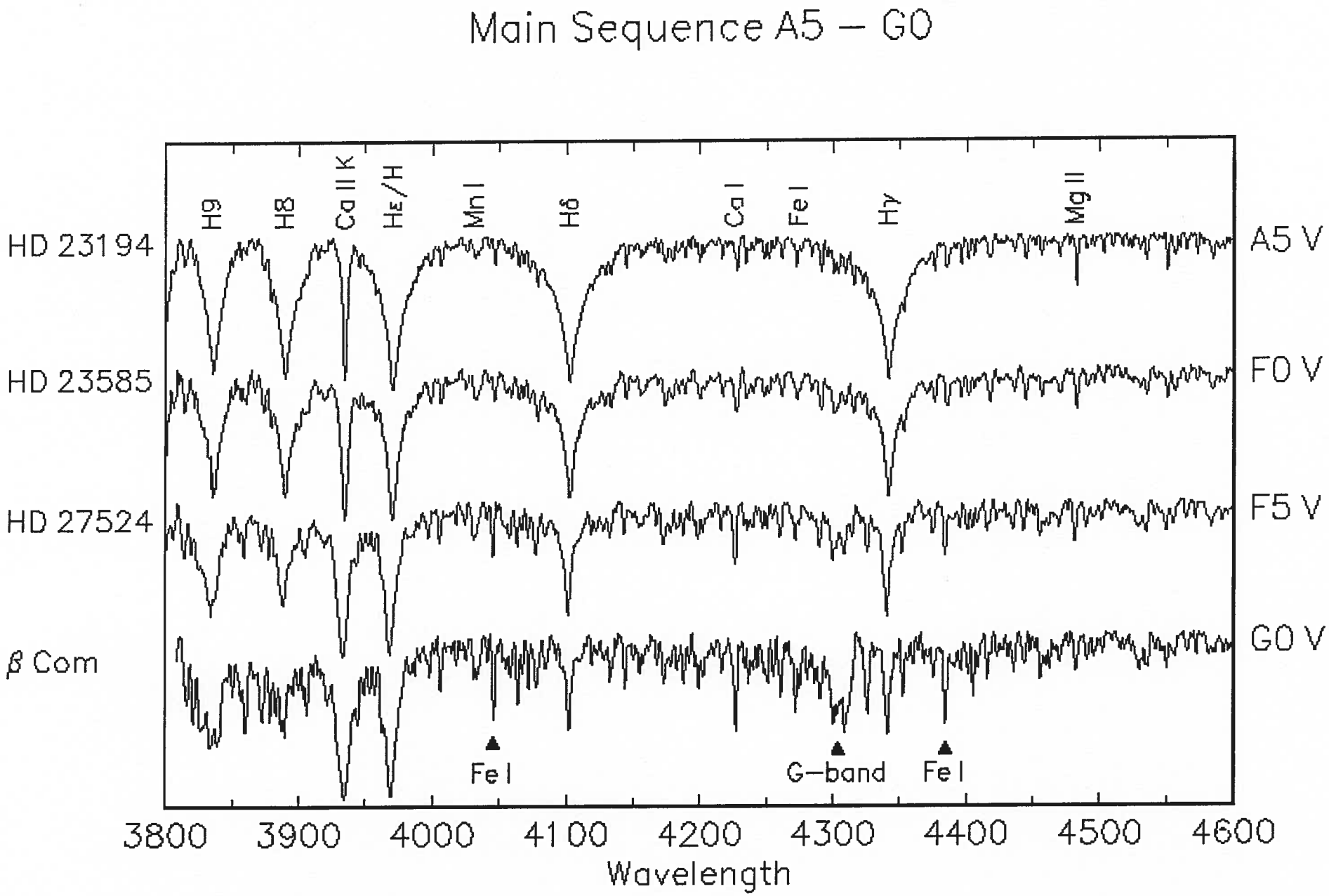
Main Sequence A5 – G0
Hθ
H8
Ca II K
Hε/H
Mn I
Hδ
Ca I
Fe I
Hγ
Mg II
HD 23194
HD 23585
HD 27524
β Com
A5 V
F0 V
F5 V
G0 V
Fe I
G–band
Fe I
3800
3900
4000
4100
4200
4300
4400
4500
4600
Wavelength

Main Sequence G0 – K5

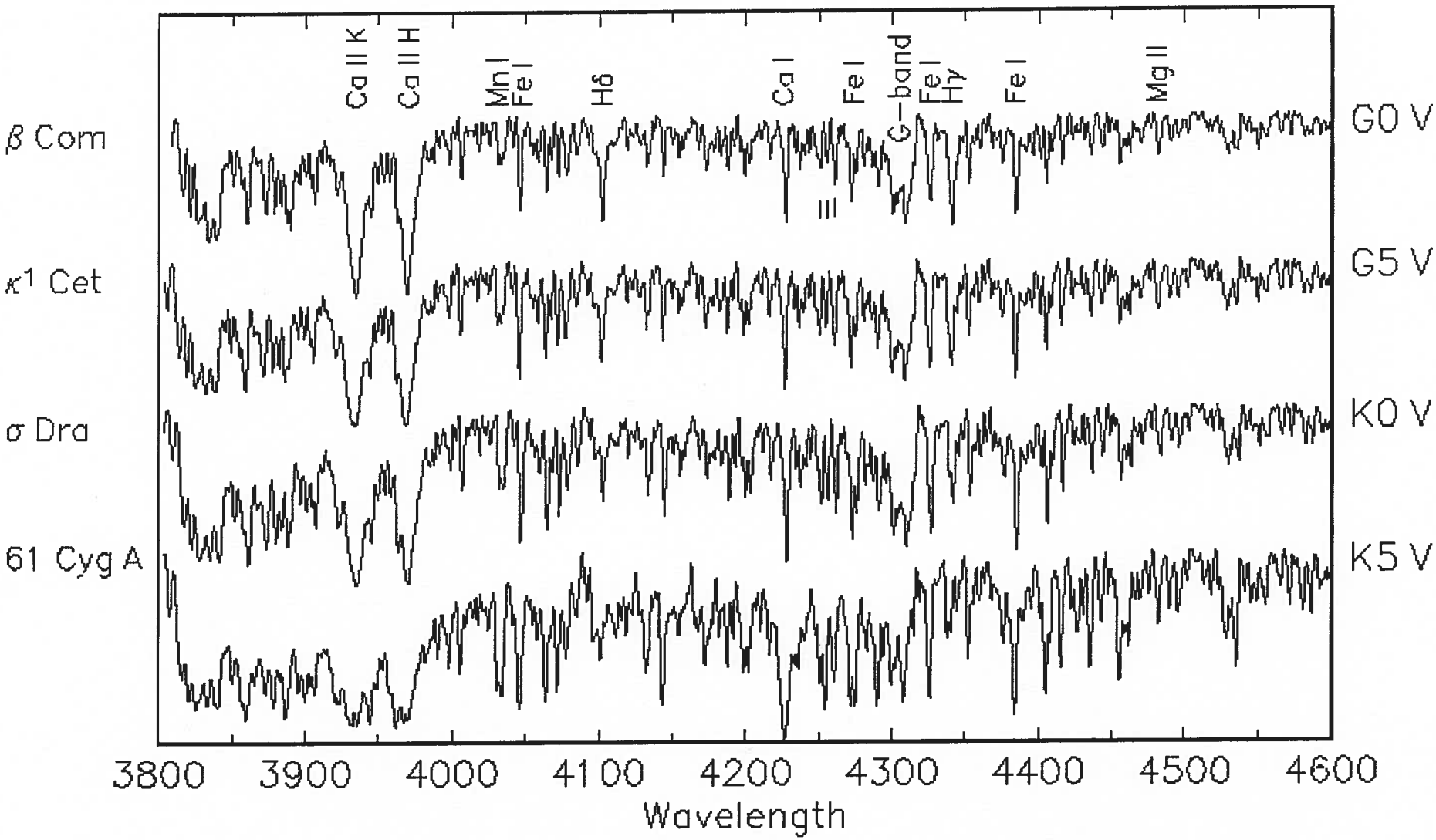

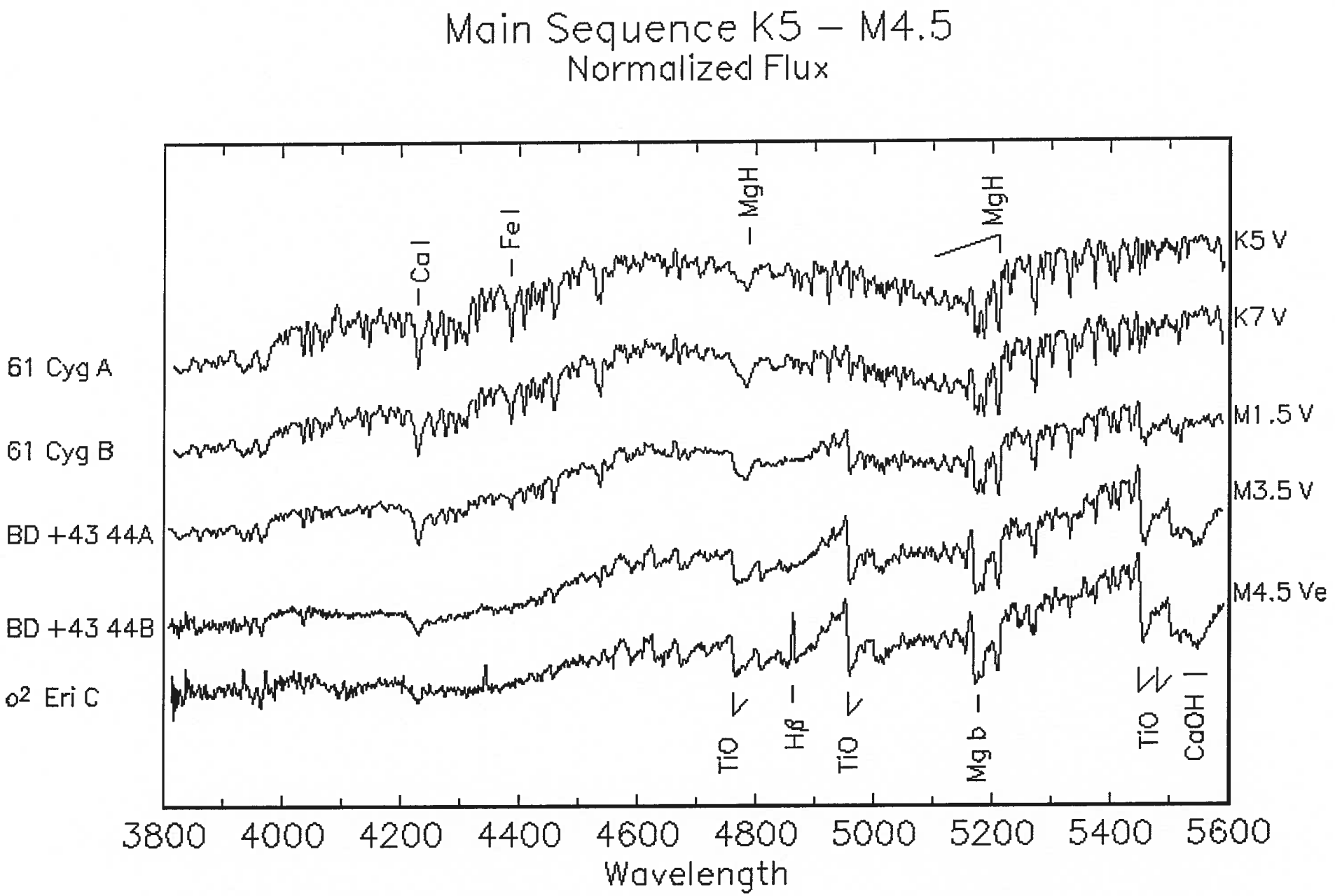
Main Sequence K5 – M4.5
Normalized Flux
Ca I
Fe I
MgH
MgH
K5 V
K7 V
M1.5 V
M3.5 V
M4.5 Ve
61 Cyg A
61 Cyg B
BD +43 44A
BD +43 44B
o2 Eri C
TiO
Hβ
TiO
Mg b
TiO
CaOH
3800
4000
4200
4400
4600
4800
5000
5200
5400
5600
Wavelength

Luminosity Effects at A0

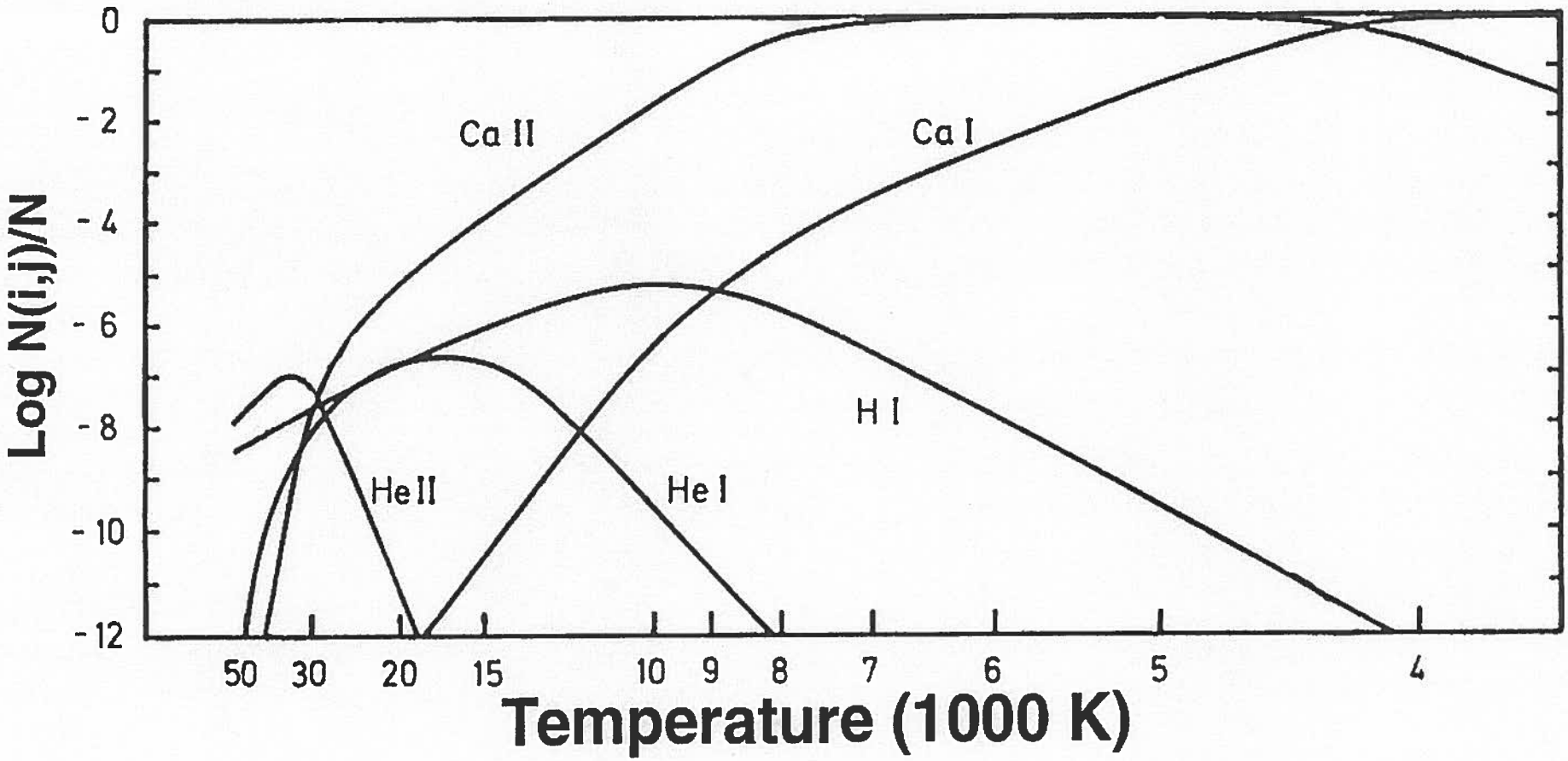
0
- 2
- 4
- 6
- 8
- 10
- 12
Log N(i,j)/N
Ca II
Ca I
H I
He II
He I
50
30
20
15
10
9
8
7
6
5
4
Temperature (1000 K)

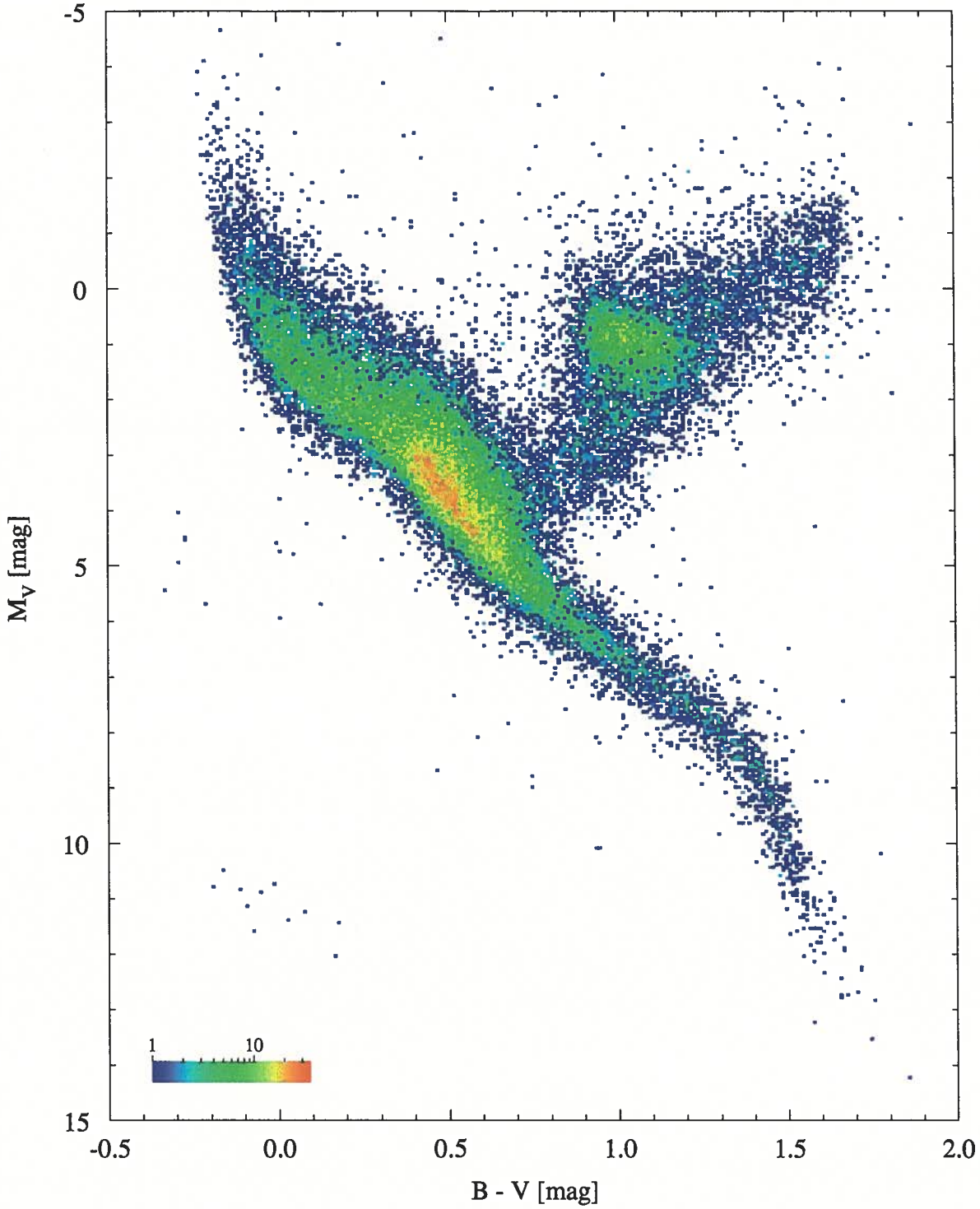
-5
0
5
10
15
M_V [mag]
-0.5
0.0
0.5
1.0
1.5
2.0
B - V [mag]
1
10

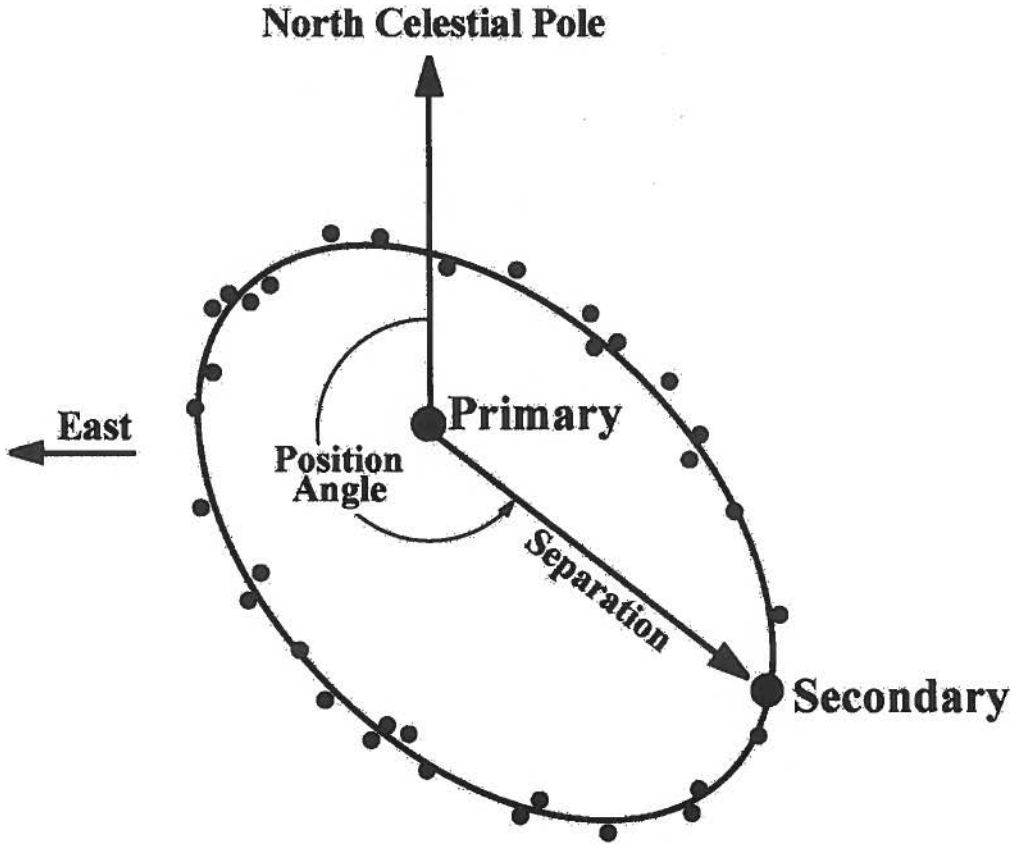
North Celestial Pole
East
Primary
Position
Angle
Separation
Secondary

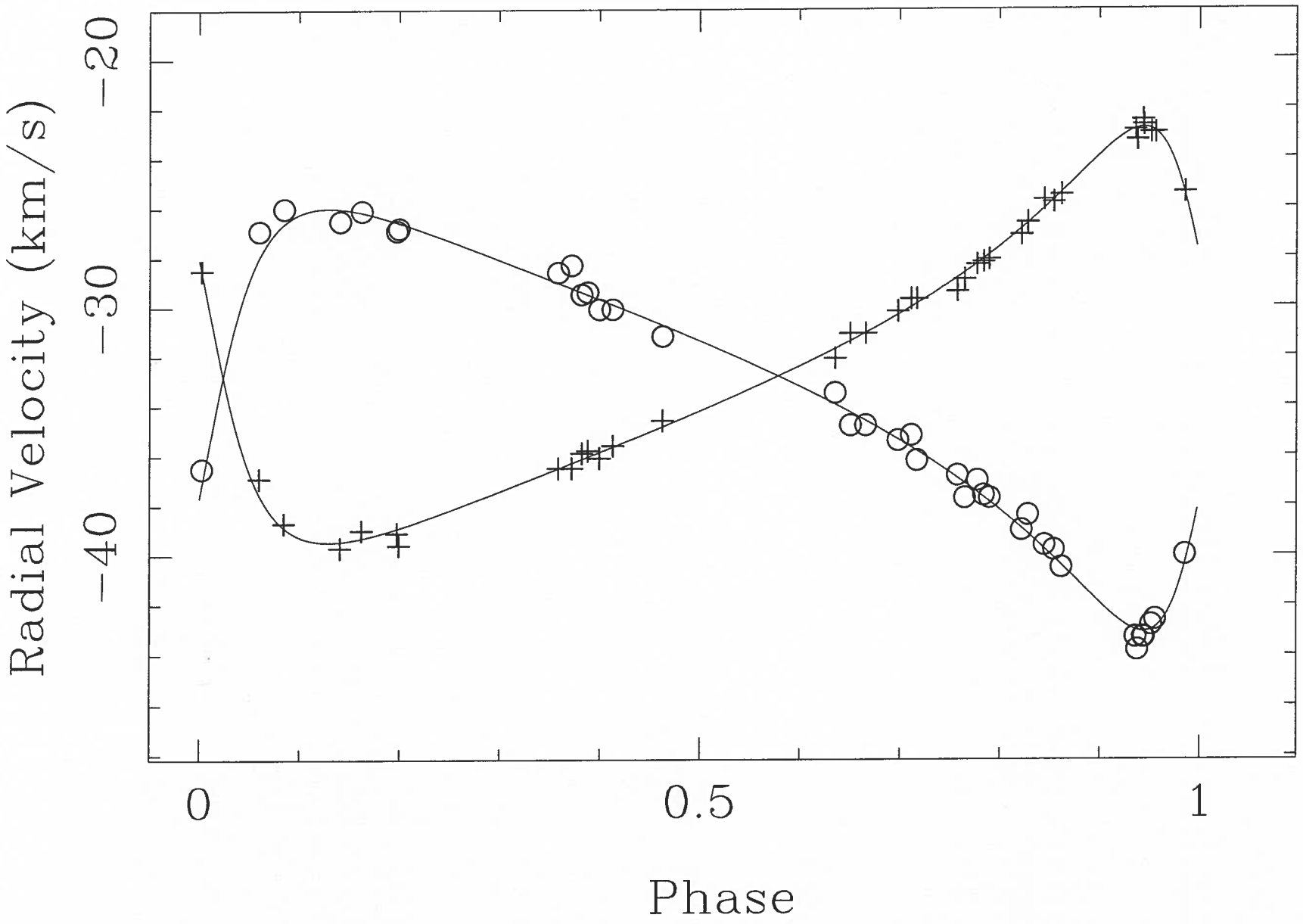
Velocity Curve for HR 7955
Radial Velocity (km/s)
−20
−30
−40
0
0.5
1
Phase

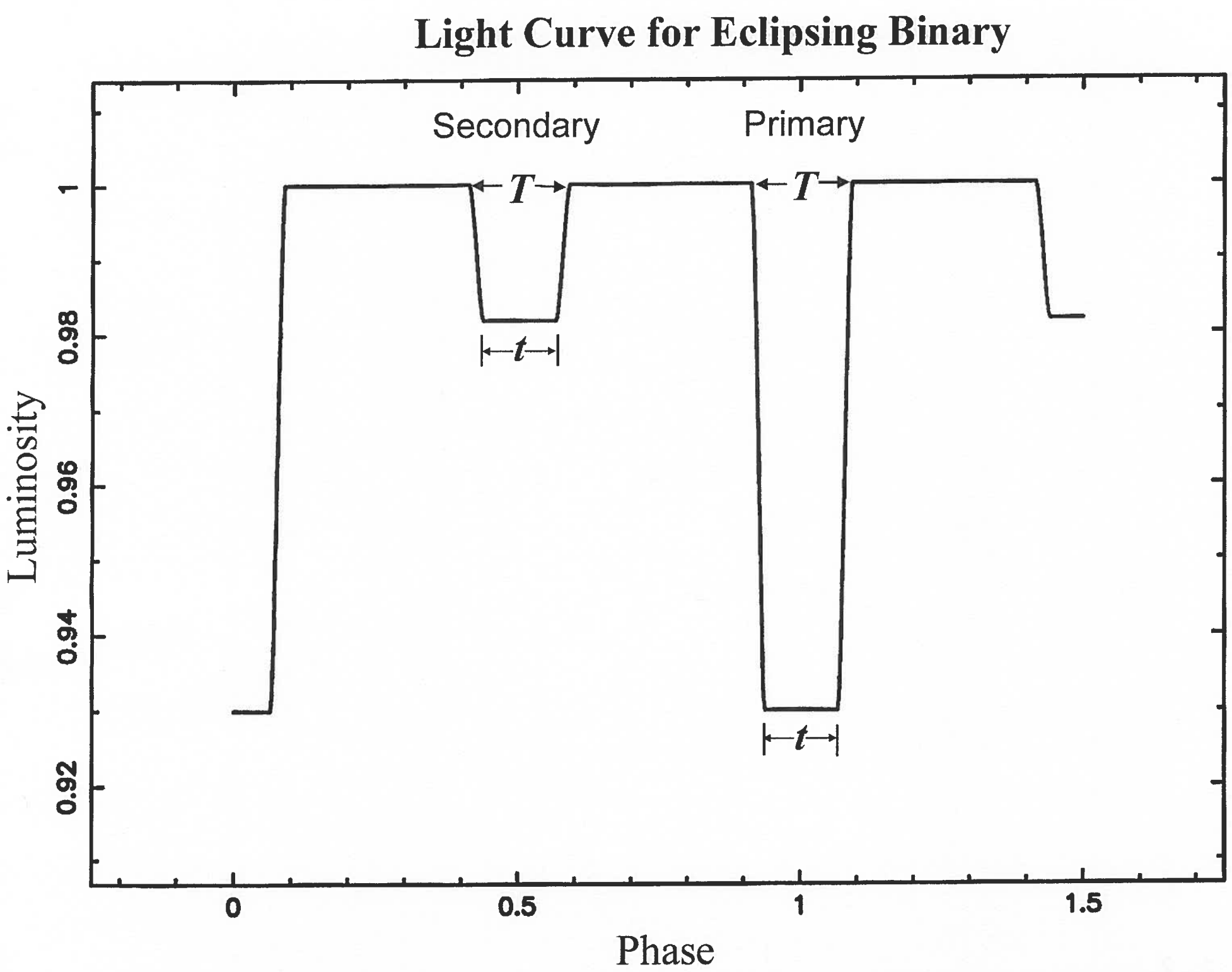
Light Curve for Eclipsing Binary
Secondary
Primary
T
T
t
t
Luminosity
1
0.98
0.96
0.94
0.92
0
0.5
1
1.5
Phase

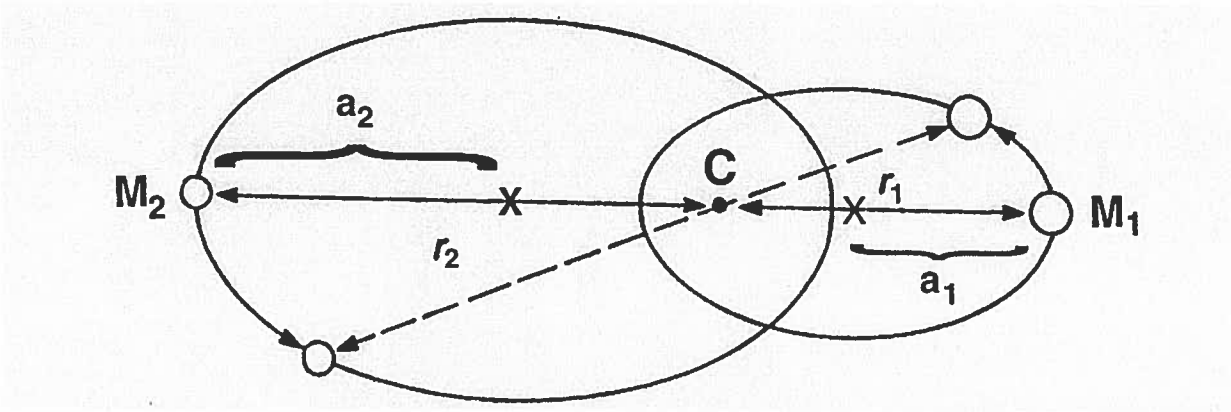
a2
M2
C
r1
M1
r2
a1

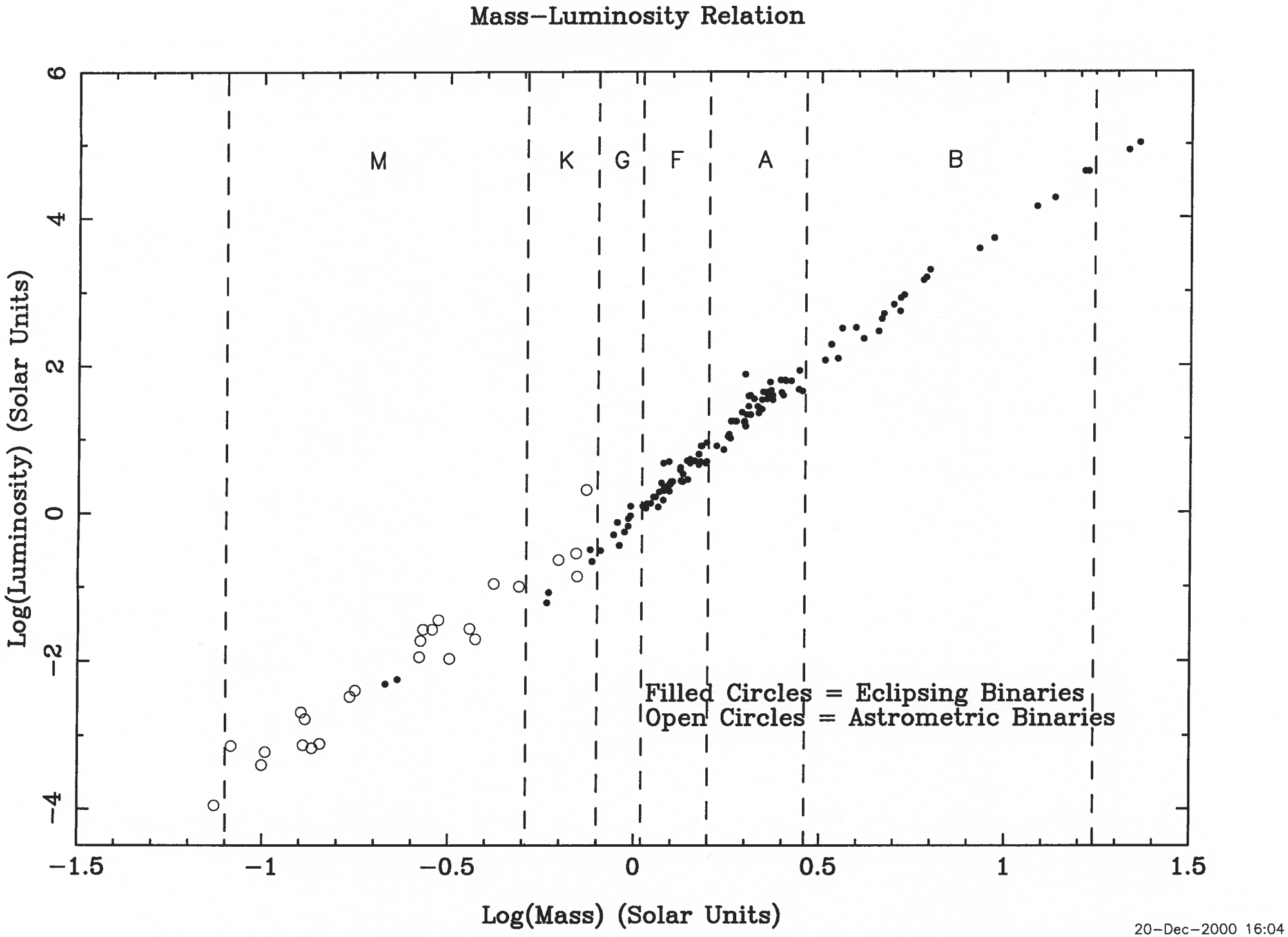
Mass–Luminosity Relation
M
K
G
F
A
B
Filled Circles = Eclipsing Binaries
Open Circles = Astrometric Binaries
Log(Luminosity) (Solar Units)
Log(Mass) (Solar Units)
6
4
2
0
−2
−4
−1.5
−1
−0.5
0
0.5
1
1.5
20–Dec–2000 16:04